Compromised Controller Design for Current Sharing and Voltage Regulation in DC Microgrid

Han, Renke; Wang, Haojie; Jin, Zheming; Meng, Lexuan; Guerrero, Josep M.

Published in:
IEEE Transactions on Power Electronics

DOI (link to publication from Publisher):
10.1109/TPEL.2018.2878084

Publication date:
2019

Document Version
Accepted author manuscript, peer reviewed version

This article has been accepted for publication in a future issue of this journal, but has not been fully edited. Content may change prior to final publication. Citation information: DOI 10.1109/TPEL.2018.2878084, IEEE Transactions on Power Electronics

Compromised Controller Design for Current Sharing and Voltage Regulation in DC Microgrid

Renke Han, *Member, IEEE*, Haojie Wang, Zheming Jin, *Student Member, IEEE*, Lexuan Meng, *Member, IEEE*, Josep M. Guerrero, *Fellow, IEEE*

***Abstract*— Since a dc Micro-Grid consists of power converters connected through different line impedances, tuning of the voltage controller provides a simple and intuitive tradeoff between the conflicting goals of voltage regulation and current sharing. A highly flexible distributed control strategy is proposed to achieve balanced control between the two control objectives, which includes the containment-based voltage controller and consensus-based current controller. The terminal voltage can be bounded within a prescriptive range which means each terminal voltage is controllable instead of only controlling the average voltage, meanwhile the current sharing performance can be regulated among converters. The two objectives, including either bounding voltages tightly or decreasing current sharing errors, can be compromised between each other by tuning the weightings of controllers. The large signal model is developed to analyze the tuning principle about different control parameters. The proposed strategy can provide flexible control performance according to various control requirements. Experimental results and comparisons are illustrated to verify the effectiveness of the proposed method and compromised tuning under resistive loads and constant power loads (CPL), dynamic voltage boundary conditions.**

***Index Terms* — Compromised controller design, Containment/consensus-based distributed controller, voltage bound, current sharing, large signal model, stability analysis.**

I. Introduction

With the increasing penetration of renewable energy sources into modern electric grid, the concept of Micro-Grid (MG) is identified as an effective method for power generation and distribution [1] [2] [3]. Since no reactive power, transformer inrush current, or harmonics issues exist in dc power grid, the dc nature of emerging renewable energy sources lends itself to a dc MG paradigm [4] [5] [6] with higher power quality and system efficiency [7] [8]. Control strategies for dc MGs can be broadly categorized into two groups, namely, constant dc voltage control schemes also called master-slave control scheme [9] [10] and droop control schemes. The main drawback of the master-slave scheme is that the operation of the entire dc MG depends upon the normal operation of one master converter, which is prone to the single point of failure. By applying the droop-controlled scheme, multiple converters are operated cooperatively to regulate the bus voltage, meanwhile it is better for converters to provide power proportional to their power capacities avoiding overloaded or unreliability. Similar to the reactive power-voltage droop control (*Q*-*V*) in ac MG [11] [12], the output voltages in dc MGs can deviate from the nominal value. In addition, when implementing *V*-*I*/*I*-*V* droop controller [13], since no global measured information exist for bus voltages due to the different line impedances, the accurate current sharing cannot be achieved. Especially when operating dc sources with long feeders in low voltage dc MGs, the voltage droop and inaccuracy of current sharing are becoming more serious.

To improve the accuracy of the current sharing, a state-of-charge (SoC) based droop control is proposed for dc energy storage system [14], in which the droop parameter is inversely proportional to the *n*th order of SoC to balance the output power between different energy storage units. In [15], another SoC-based adaptive virtual impedance is proposed to improve the transient current sharing among the parallel supercapacitors without physical communication. Both two methods are considering the resistive loads without line impedances in the system and the voltage at the point of common coupling (PCC) is deviated from the nominal value due to the droop control effects. In [16] and [17], another two adaptive droop controllers based on a superimposed frequency is proposed, by which the load sharing accuracy is improved for both resistive loads and constant power loads (CPL). However, due to the superimposed small ac voltage, oscillations existing in the output voltages and currents affect the system power quality. From stability enhancement point of view, the plug-and-play (PnP) controller [18] [19] conception is proposed to guarantee the global voltage stability of the whole system; however, the problem of current sharing is not considered.

To consider both the current sharing and voltage regulation simultaneously, centralized [20] [21], and distributed, [22]-[34] controllers in secondary control level are proposed based on the hierarchical control structure. In [20], by sensing and transmitting the PCC voltage, the centralized secondary controller is proposed to restore PCC voltage. When the line impedance differences are not large, the current sharing can be approximately achieved by droop controller. In [21], for more electric aircrafts (MEA), a global voltage droop conception is proposed to achieve PCC voltage restoration and accurate current sharing. However, when one converter is failure, the

Manuscript received May 26, 2018; revised Aug. 31, 2018; accepted Oct. 15, 2018. Paper has been presented at the 2017 IEEE Energy Conversion Congress and Exposition (ECCE), Cincinnati, Oct. 1-5, USA [1]. (*Corresponding author: Renke Han*.)

R. Han, Z. Jin, L. Meng, and J. M. Guerrero are with Department of Energy Technology, Aalborg University, 9220, Aalborg, Denmark (e-mail: rha@et.aau.dk, zhe@et.aau.dk. lexuan.meng@gmail.com, joz@et.aau.dk).

H. Wang is with Global Energy Interconnection Corporation, 100031, Beijing, China. (e-mail: haojie-wang@geidco.org).

This article has been accepted for publication in a future issue of this journal, but has not been fully edited. Content may change prior to final publication. Citation information: DOI 10.1109/TPEL.2018.2878084, IEEE Transactions on Power Electronics

TABLE I. Comparison of secondary control for a dc Microgrid in the literature

Secondary controller	Control architecture					Control objectives		
	Centralized Controller	Decentralized Controller	Distributed Controller			Around nominal voltage	Average voltage	Accurate current sharing
			Optimization-based	Dynamic *consensus*-based	Static *PI*-based			
Guerrero et al. [20]	√	-	-	-	-	√	-	-
Gao et al. [21]	√	-	-	-	-	√	-	√
Mokhtar et al. [25]	-	-	-	-	√	√	-	√
Anand et al. [22]	-	-	-	-	√	-	-	√
Lu et al. [23]	-	-	-	-	√	-	√	√
Huang et al. [24]	-	-	-	-	√	-	√	-
Wang et al. [26]	-	-	-	-	√	-	√	√
Peyghami et al. [16] [17]	-	√	-	-	-	√	-	√
Augustine et al. [35]	-	-	√	-	-	-	-	√
Ingle et al. [36]	-	-	√	-	-	-	-	√
Han et al. [33]	-	-	-	√	-	-	-	√
Nasirian et al. [29] [30]	-	-	-	√	-	-	√	√
Sahoo et al. [31]	-	-	-	√	-	-	√	√
Cucuzzella et al. [32]	-	-	-	√	-	-	√	√

global voltage droop parameter needs to be updated. If not, the voltage control performance will be compromised. From system-level viewpoint, loss of any communication link or electrical link in such centralized controllers can lead to the failure of the corresponding unit, and potentially lead to instability and cascaded failures. A distributed control [22] is proposed to achieve the per-unit current sharing by calculating the average current value. Then, by using both the average voltage and current values, an improved droop control in [23] is proposed to achieve the current sharing and restore the dc bus voltages, which is developed for two-converter system. The similar method from [20] is modified in a distributed sense [24] to restore average output voltages as the pilot bus regulation by only using the average voltage value, meanwhile the equal current sharing can be approximately achieved when the line impedance differences are not large. Meanwhile, the similar idea is redesigned by combining sliding mode inner-loop controller in [25]. Furthermore, in [26], based on the average droop parameters, average output currents and average voltages, the droop control curve is adjusted to achieve current sharing and average voltage regulation. In above distributed methods, the accurate current sharing is considered as the main objective; for voltage regulation, there are two options, one of which is to fix PCC voltage at nominal value, another of which is to control output voltages around nominal value as an ancillary objective without a specific value. In addition, since all the converters share related information through one communication bus, large amounts of communication sources are needed to share the average information, which can degrade the reliability of the communication bus.

Recently, the consensus-based distributed control conception [27] [28] has emerged as an attractive alternative; if designed properly it can offer improved reliability, simplified communication topology, reduced communication traffic and enhanced scalability. Combined with the consensus-based communication protocol [27], a voltage observer [29] is proposed to estimate the average voltage value generating a voltage correction term, meanwhile the consensus-based current regulator provides a resistance correction term. Then, a noise-resilient voltage observer combined with consensus-based voltage/current regulator is proposed to achieve more resiliency control in dc MGs [30]. Both two above methods can control the average output voltage equal to nominal value and achieve the accurate current sharing proportionally. Then, the similar idea is extended by [31] [32] which can guarantee the convergence of the system within the finite time. In terms of the communication traffic reduction, an event-triggered-based distributed current sharing controller is proposed [33] and then the communication delay effects are further considered in [34]. For the consensus-based control method mentioned above, the accurate current sharing can still be achieved, and the average value of output voltages is fixed at nominal value.

From the optimization viewpoint, the droop index (DI) conception is proposed in [35] to minimize the current sharing error and power losses by tuning droop parameters. However, the line impedance information is needed to calculate the power losses. Later, a quality-index [36] is proposed by calculating the current sharing errors and voltage drops, based on which the optimization problem is formed to find optimal droop parameters minimizing the quality-index. However, the system dynamic performance and stability is sensitive to the droop parameters. Meanwhile, since no specific voltage boundary is given for optimal controller, it is not suitable for different operating conditions, especially with large line impedance

This article has been accepted for publication in a future issue of this journal, but has not been fully edited. Content may change prior to final publication. Citation information: DOI 10.1109/TPEL.2018.2878084, IEEE Transactions on Power Electronics

differences.

To conclude above discussion and comparison, the existing secondary control methods in dc MG are summarized in Table I. It can be concluded that the main objective for most of the methods is to achieve the accurate current sharing under different circumstances. Meanwhile, in the voltage control sense, they are devoted to either restore the PCC voltage or fix the average voltages at the nominal value.

Nevertheless, converters or load terminal voltages are also of great importance. It should be noted that if the differences of line impedances are considerably large, only fixing the average voltage value at nominal value cannot guarantee that the individual terminal voltage is kept within the standard limits. From the perspective of power flow in a dc MG, the terminal voltage from each converter should exist deviations around the nominal value, otherwise there is no power flow in the system [37]. On the other hand, large voltage deviations can cause stability problems and destroy power quality according to the standard in [38] [39]. Furthermore, the power quality and stability margin for local load will be worse than before due to the voltage deviations. To solve the above-mentioned challenges, this paper presents a compromised control conception between current sharing and voltage regulation to balance the trade-off and satisfy different requirements. The main contributions of this paper are considered in the following aspects:

1). Compromised control conception is proposed to achieve balanced control between voltage regulation and current sharing among power converters.

2). The containment-based controller is proposed to bound voltages within a reasonable range and keep necessary voltage deviations for power flow regulation. Meanwhile, the consensus-based current controller is implemented to guarantee current sharing to a certain degree.

3). According to different system requirements and conditions, the performance including tighter voltage bound or more accurate current sharing can be compromised between each other through tuning control weightings.

4). The large signal model including the proposed controller and the electrical topology of the dc MG is established to analyse the sensitivity and tuning principles of control parameters.

5). The experimental results and comparison with existing literatures are shown to verify the effectiveness of the proposed method.

The paper is organized as follows. In Section II, the compromised control conception is proposed by introducing containment and consensus-based distributed coordination control strategy. In Section III, the large signal model and its stability analysis are provided. In Section IV, experimental results are presented to prove the effectiveness of proposed controller. Finally, the paper is concluded in Section V.

II. Compromised Controller in Reverse Droop based DC MG

This section explains proposed compromised controllers based on the hierarchical control structure for a dc MG. The reverse droop control is explained in the primary control level. Furthermore, the proposed containment-based voltage controller and consensus-based current controller is explained in detail in the secondary control level to form the compromised controller.

A. Definitions and Notations

For the control system with n distributed controllers, a controller is called a *leader* if it only provides information to its neighbors and does not receive information. A controller is called a *follower* if it can receive/send information from/to one or more neighbors through communication topology. Let N_i denote the set of i_{th}-controller neighbors chosen from followers, and R_i as the set of leaders which can give its information to i_{th}-agent directly. This definition is applied to containment-based voltage controller, in which the dynamic range is appointed in charge of setting the lower and upper voltage boundaries respectively. Meanwhile, the consensus-based current controller only uses the neighbors' information without the reference leaders' information.

Let C be a set in a real vector space $V \subseteq R^p$. The set C is called convex if, for any x and y in C, the point $(1-z)x+zy$ is in C for any $z\in[0,1]$. The convex hull for a set of points $X=\{x_1,\ldots,x_q\}$ in V is the minimal convex set containing all points in X. Let $Co(X)$ denote the convex hull of X. In particular, when $V \subseteq R$, $Co(X)=\{x|x\in[\min x_i, \max x_i]\}$ which will be used in this paper. In addition, define vector $Z\in R^n$, then $diag(Z)\in R^{n\times n}$ as the diagonal matrix whose diagonal elements are the elements in vector Z. I_n is the unit matrix and $0_{[n]}$ is the zero $n\times n$ matrix. 0_n and 1_n are the n-vectors with all 0 and 1 elements.

For the consensus-based current controller, an adjacency matrix is defined as $A=[a_{ij}]\in R^{n\times n}$ with $a_{ij}=1$ if node i can receive information from node j otherwise $a_{ij}=0$; The Laplacian matrix is defined as $L_I=\left[l_{ij}\right]\in R^{n\times n}$ with $l_{ii}=\sum_{j=1}^{n}a_{ij}$ and $l_{ij}=-a_{ij}, i\neq j$. For the containment-based controller, another adjacency matrix is defined as $B=\left[b_{ij}\right]\in R^{n\times 2}$ with $b_{il}=1$ if node i can receive information from one of the two reference leaders otherwise $b_{il}=0$, in which l represents the label of two reference leaders; Another matrix is defined as $L_V^{'}=\left[l_{ij}\right]\in R^{n\times(n+2)}$ with $l_{ii}=\sum_{j=1}^{n}a_{ij}+\sum_{l=n+1}^{n+2}b_{il}$; for other items, when $j<n$, $l_{ij}=-a_{ij}$, otherwise when $j>n$, $l_{ij}=-b_{ij}$. For convenience, the matrix $L_V^{'}$ is divided into $L_V^{'}=\left[L_V \quad L_{Bou}\right]$ in which $L_V\in R^{n\times n}$ and $L_{Bou}\in R^{n\times 2}$.

The adjacency matrix represents the communication topology mathematically. From the graph theory viewpoint, for the consensus-based current controller, since only followers communicate with their neighbors, the communication topology needs to be connected graph. For the containment-based voltage controller, there are several followers and two leaders in the system, the communication topology among followers needs to be connected graph which is same as before, meanwhile the communication topology between followers and leaders should contain at least a spanning tree to make sure that all the followers can receive the information from one of the leaders at least indirectly. For rigorous theoretical proof

This article has been accepted for publication in a future issue of this journal, but has not been fully edited. Content may change prior to final publication. Citation information: DOI 10.1109/TPEL.2018.2878084, IEEE Transactions on Power Electronics

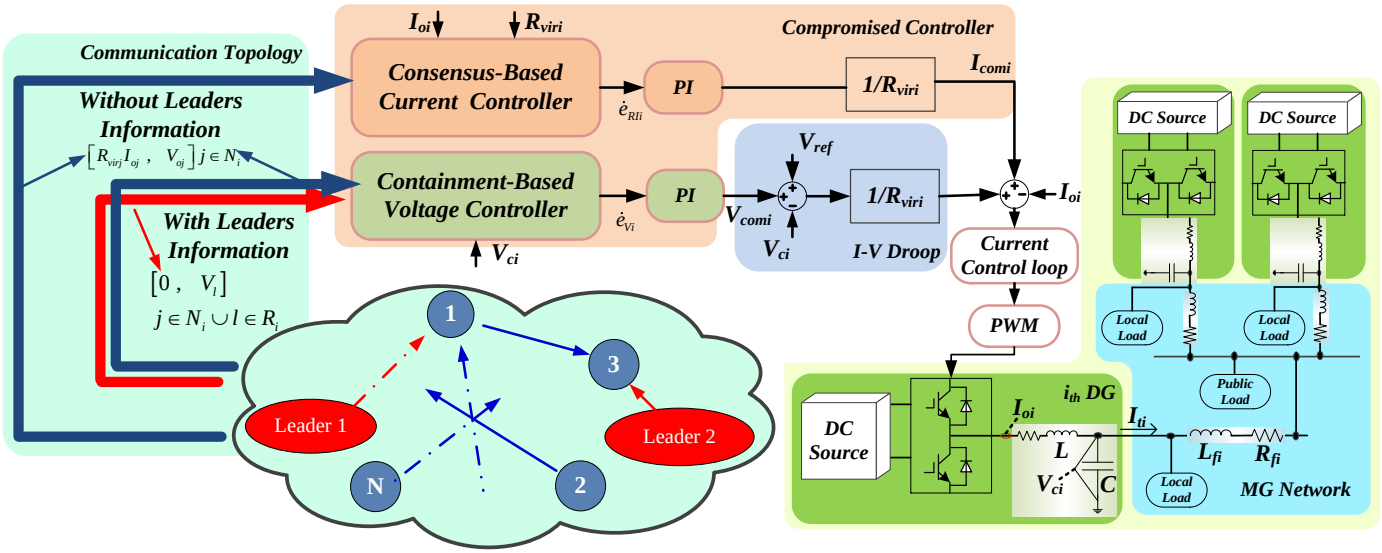

Fig. 1. Configuration of the compromised controller in a dc MG.

mathematically, the consensus-based algorithm can be referred in [27] and the containment-based algorithm can be referred in [28].

B. Reverse Droop in the Primary Control Level

To acquire fast-dynamic response, the single current *PI* control loop is used to replace the voltage and current double control loop. Thus, the reverse droop controller is implemented to replace the outer voltage control loop, which is

$$I_{refi} = \frac{V_{ref} - V_{ci}}{R_{viri}} \tag{1}$$

where I_{refi} is the current reference for current *PI* controller, R_{viri} is the virtual resistance, V_{ci} is the output voltage measured from the output capacitor.

As discussed before, in the primary level, due to the different line impedances, the current sharing performance is inaccurate, and the output voltages drop from the nominal value. In the next subsection, to solve the trade-off effect between the conflicting goals of voltage regulation and current sharing in the secondary control level, a containment and consensus-based controller is proposed to form a compromised control conception between the two conflicting goals accordingly.

C. Containment and Consensus-based Controller in the Secondary Control Level

The containment-based voltage controller generates a correction item e_{Vi} for each converter to bound voltages within a reasonable range. The range in the algorithm is formed by upper bound V_{Ubou} and lower bound V_{Lbou}. The controller is defined as:

$$\dot{e}_{Vi} = w_v\left(-\sum_{j\in N_i} a_{ij}\left(V_{ci} - V_{cj}\right) - \sum_{l\in R_i} b_{il}\left(V_{ci} - V_{bou}\right)\right) \tag{2}$$

where V_{bou} is the voltage boundary reference which can be either upper boundary V_{Ubou} or lower boundary V_{Lbou}, w_v is the weighting for containment-based controller, which is assumed that the weighting of voltage controller for all the converters is same.

Remark 1: In a containment-based voltage controller, at least one converter should receive the lower boundary directly, meanwhile at least one converter can receive the upper boundary directly.

Eq. (2) can be written into matrix formation as

$$\dot{e}_V = w_v\left(-L_V V_C - L_{Bou} V_{Bou}\right) \tag{3}$$

where $e_V = [e_{V1} \ \cdots \ e_{Vn}]^T$, $V_C = [V_{c1} \ \cdots \ V_{cn}]^T$, $V_{Bou} = [V_{Ubou} \ \ V_{Lbou}]^T$.

Then $\dot{e}_{Vi}$ is fed into a *PI* controller defined as: $G_{Vi} = k_{pVi} + k_{iVi}/s$ in which s is the Laplace operator. Then the compensating item from containment-based voltage controller for i_{th} DG can be written as

$$V_{comi} = k_{pVi}\dot{e}_{Vi} + k_{iVi}e_{Vi} \tag{4}$$

The consensus-based current controller generates correction item e_{RIi} for current compensation for each converter, which can be written as:

$$\dot{e}_{RIi} = w_c\left(-\sum_{j\in N_i} a_{ij}\left(R_{viri}I_{oi} - R_{virj}I_{oj}\right)\right) \tag{5}$$

where I_{oi} is the total output current from i_{th} converter, w_c is the weighting for consensus-based voltage controller.

Eq. (5) can be rewritten into matrix formation as

$$\dot{e}_{RI} = w_c\left(-L_I R_{vir} I_O\right) \tag{6}$$

where $e_{RI} = [e_{RI1} \ \cdots \ e_{RIn}]^T$, $R_{vir} = diag\left\{[R_{vir1}, \ \cdots \ R_{virn}]^T\right\}$, $I_O = [I_{o1} \ \cdots \ I_{on}]^T$.

Then $\dot{e}_{RIi}$ is fed into another *PI* controller: $G_{Ii} = k_{pIi} + k_{iIi}/s$. The compensating item from consensus-based current controller for i_{th} converter is written as

$$I_{comi} = \frac{1}{R_{viri}}\left(k_{pIi}\dot{e}_{RIi} + k_{iIi}e_{RIi}\right) \tag{7}$$

By adding the proposed voltage and current control shown in eq. (4) and (7), eq. (1) can be changed as

$$I_{refi} = \frac{V_{ref} - V_{ci} + V_{comi}}{R_{viri}} + I_{comi} \tag{8}$$

This article has been accepted for publication in a future issue of this journal, but has not been fully edited. Content may change prior to final publication. Citation information: DOI 10.1109/TPEL.2018.2878084, IEEE Transactions on Power Electronics

Here, the total control input for each converter from the secondary control level is calculated as $\left(V_{comi}+I_{comi}R_{viri}\right)$ whose value will be shown in the experimental results in Section IV.

The configuration of proposed compromised controller is shown in Fig. 1 including the reverse droop controller, the containment-based voltage controller, and the consensus-based current controller.

To be emphasized, the compromised control weightings w_v and w_c can be tuned according to different requirements. We will show the tuning principle in the next section.

III. Large Signal Model and Parameters Design

This section develops the large signal model for control and weighting parameters design guideline. The model includes proposed containment-based voltage controller and consensus-based current controller, reverse droop control, inner current control, electrical model for a dc MG.

A. Modeling for the System with Proposed Controllers

Combining eq. (4) with (7), the eq. (8) can be rewritten as

$$I_{refi}=\frac{V_{ref}-V_{ci}+\overbrace{k_{pVi}\dot{e}_{Vi}+k_{iVi}e_{Vi}}^{V_{comi}}}{R_{viri}}+\overbrace{\frac{1}{R_{viri}}\left(k_{pIi}\dot{e}_{RIi}+k_{iIi}e_{RIi}\right)}^{I_{comi}} \quad (9)$$

Combining eq. (3) with (6), eq. (9) can be rewritten as (matrix formation)

$$I_{Ref}=R_{vir}^{-1}\begin{bmatrix}V_{Ref}-V_C+K_{pV}w_v\left(-L_VV_C-L_{Bou}V_{Bou}\right)\\+K_{iV}e_V+K_{pI}w_c\left(-L_IR_{vir}I_O\right)+K_{iI}e_{RI}\end{bmatrix} \quad (10)$$

where $K_{pV}=diag\left(\begin{bmatrix}k_{pV1} & \cdots & k_{pVn}\end{bmatrix}^T\right)$,

$K_{iV}=diag\left(\begin{bmatrix}k_{iV1} & \cdots & k_{iVn}\end{bmatrix}^T\right)$, $K_{iI}=diag\left(\begin{bmatrix}k_{iI1} & \cdots & k_{iIn}\end{bmatrix}^T\right)$,

$K_{pI}=diag\left(\begin{bmatrix}k_{pI1} & \cdots & k_{pIn}\end{bmatrix}^T\right)$, $I_{Ref}=\begin{bmatrix}I_{ref1} & \cdots & I_{refn}\end{bmatrix}^T$,

$R_{vir}=diag\left(\begin{bmatrix}R_{vir1} & \cdots & R_{virn}\end{bmatrix}^T\right)$, $V_{Ref}=1_nV_{ref}$.

To make eq. (10) more clearly, it can be rewritten as

$$\begin{aligned}I_{Ref}=&R_{vir}^{-1}\left(-I_n-K_{pV}w_vL_V\right)V_C-R_{vir}^{-1}K_{pI}w_cL_IR_{vir}I_O\\&+R_{vir}^{-1}K_{iV}e_V+R_{vir}^{-1}K_{iI}e_{RI}\\&+R_{vir}^{-1}V_{Ref}-R_{vir}^{-1}K_{pV}w_vL_{Bou}V_{Bou}\end{aligned} \quad (11)$$

Since the inner current loop is much faster than the outer control loop, the inner current loop *PI* controller combining with the output inductor and its equivalent resistance can be simplified by a first-order lag as

$$G_C\left(s\right)=\frac{1}{\tau s+1} \quad (12)$$

where $1/\tau$ is the equivalent control bandwidth for the equivalent part.

Thus, the relationship between I_{refi} and I_{oi} can be written as

$$I_{oi}=\frac{1}{\tau s+1}I_{refi}\xrightarrow{Matrix\ Formation}\dot{I}_O=\Gamma\left(I_{Ref}-I_O\right) \quad (13)$$

where $\Gamma=1/\tau I_n$.

Substituting eq. (11) into eq. (13), eq. (13) can be rewritten as

$$\begin{aligned}\dot{I}_O=&\Gamma R_{vir}^{-1}\left(-I_n-K_{pV}w_vL_V\right)V_C\\&+\Gamma\left(-R_{vir}^{-1}K_{pI}w_cL_IR_{vir}-I_n\right)I_O\\&+\Gamma R_{vir}^{-1}K_{iV}e_V+\Gamma R_{vir}^{-1}K_{iI}e_{RI}\\&+\Gamma R_{vir}^{-1}V_{Ref}-\Gamma R_{vir}^{-1}K_{pV}w_vL_{Bou}V_{Bou}\end{aligned} \quad (14)$$

Furthermore, the voltage boundary can be acquired through multiplying the nominal voltage V_{ref} and standard percentage *Per*. The relationship between the V_{ref} and V_{Ubou}, V_{Lbou} is written as

$$\begin{cases}V_{Ubou}=\left(1+Per\right)V_{ref}\\V_{Lbou}=\left(1-Per\right)V_{ref}\end{cases}\Rightarrow\begin{bmatrix}V_{Ubou}\\V_{Lbou}\end{bmatrix}=PV_{ref} \quad (15)$$

where $P=\begin{bmatrix}1+Per & 1-Per\end{bmatrix}^T$.

Thus, eq. (14) can be rewritten as

$$\begin{aligned}\dot{I}_o=&\Gamma R_{vir}^{-1}\left(-I_n-K_{pV}w_vL_V\right)V_C\\&+\Gamma\left(-R_{vir}^{-1}K_{pI}w_cL_IR_{vir}-I_n\right)I_O\\&+\Gamma R_{vir}^{-1}K_{iV}e_V+\Gamma R_{vir}^{-1}K_{iI}e_{RI}\\&+\left(\Gamma R_{vir}^{-1}-\Gamma R_{vir}^{-1}K_{pV}w_vL_{Bou}P\right)V_{Ref}\end{aligned} \quad (16)$$

Furthermore, due to the effects from output capacitors, the relationship among output voltage V_{ci}, total output current I_{oi} and output current I_{ti} for loads and line resistances can be modelled as

$$V_{ci}=\frac{1}{sC}\left(I_{oi}-I_{ti}\right)\xrightarrow{Matrix\ Formation}\dot{V}_C=Cap^{-1}\left(I_O-I_T\right) \quad (17)$$

In [33], it has already proven that the relationship between terminal voltage V_C and current I_T can be modelled in one matrix for any system topologies. Here, the matrix is called L_T, thus eq. (17) can be rewritten as

$$\dot{V}_C=Cap^{-1}\left(I_O-L_TV_C\right) \quad (18)$$

Combining eq. (3), (6), (16) with (18), the whole system can be written as

$$\begin{bmatrix}\dot{V}_C\\\dot{I}_O\\\dot{e}_V\\\dot{e}_{RI}\end{bmatrix}=\underbrace{\begin{bmatrix}-Cap^{-1}L_T & Cap^{-1} & 0_{[n]} & 0_{[n]}\\\Gamma R_{vir}^{-1}\left(-I_n-K_{pV}w_vL_V\right) & \Gamma\left(-R_{vir}^{-1}K_{pI}w_cL_IR_{vir}-I_n\right) & \Gamma R_{vir}^{-1}K_{iV} & \Gamma R_{vir}^{-1}K_{iI}\\-L_V & 0_{[n]} & 0_{[n]} & 0_{[n]}\\0_{[n]} & -L_IR_{vir} & 0_{[n]} & 0_{[n]}\end{bmatrix}}_{A}\begin{bmatrix}V_C\\I_O\\e_V\\e_{RI}\end{bmatrix}+\underbrace{\begin{bmatrix}0_n\\\left(\Gamma R_{vir}^{-1}-\Gamma R_{vir}^{-1}K_{pV}w_vL_{Bou}P\right)\\-L_{Bou}P\\0_n\end{bmatrix}}_{B}V_{ref} \quad (19)$$

To make the modeling process more clearly, Fig. 2 shows the equivalent model block diagram.

B. Pole-zero Loci Analysis by changing PI control parameters for Proposed Controllers

To analyze and design the parameters of *PI* controllers embedded in the proposed controllers quantitatively, a dc MG,

This article has been accepted for publication in a future issue of this journal, but has not been fully edited. Content may change prior to final publication. Citation information: DOI 10.1109/TPEL.2018.2878084, IEEE Transactions on Power Electronics

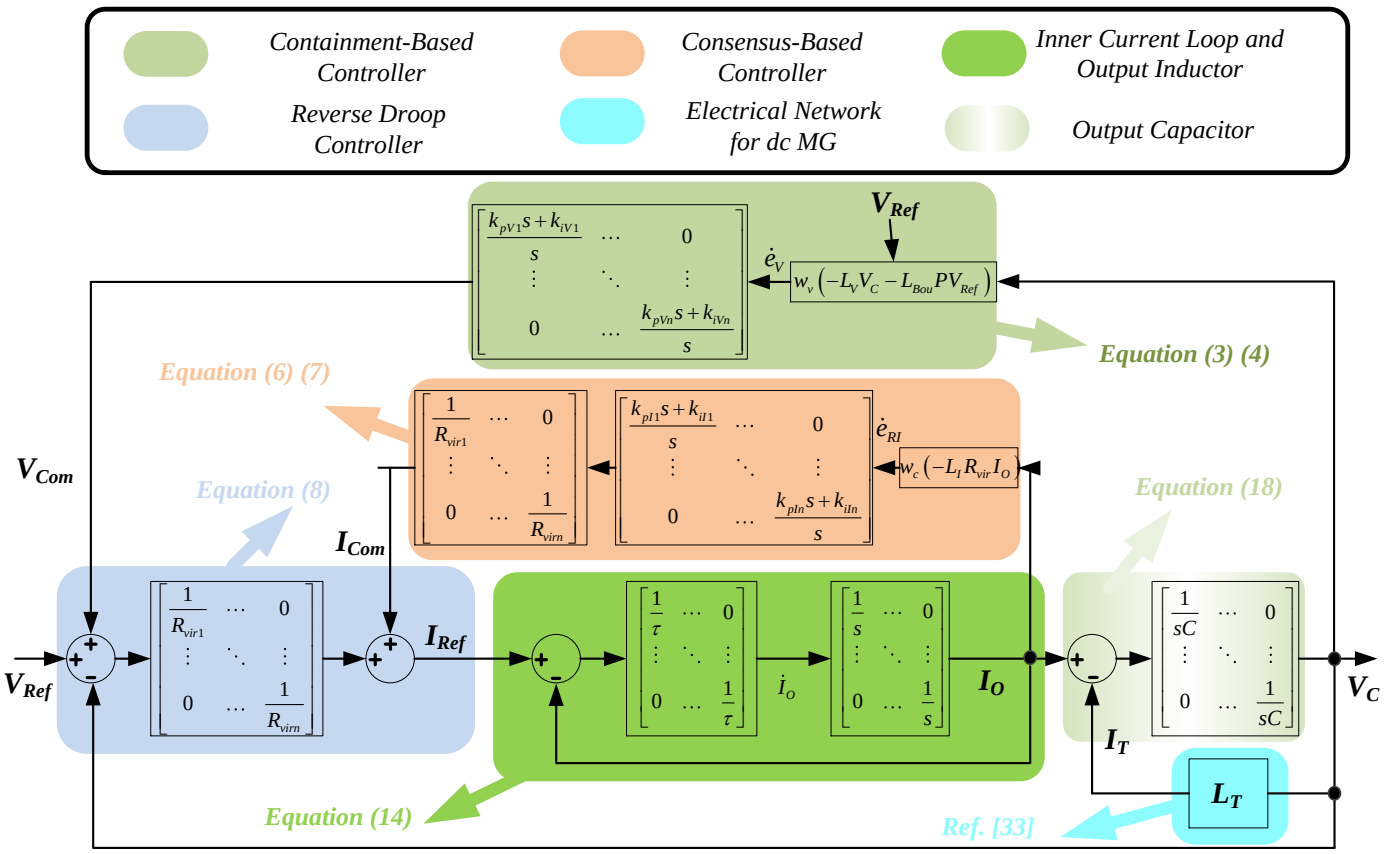

Fig. 2. Control block diagram for the whole system.

including four power converters connected by different line impedances, loads, are considered as a study case. The pole-zero loci are shown in Fig. 3 - Fig. 6 to analyze the dynamic behavior of the system.

Fig. 3 shows the pole-zero locus with the proportional parameter K_{pV} changed from 0.1 to 5 in *PI* controller for containment-based control loop. In the low frequency region, it shows in Fig. 3 (a) that by changing the proportional parameters for four converters simultaneously, a pair of dominating poles is moving away from the real axis which indicate that the system is becoming less damped. The zoomed in part of Fig. 3 (a) shows that the poles are moving towards the real axis meaning that the system is becoming less damped and the response speed is becoming slower. In the high frequency region, other pairs of poles also indicate that the system is becoming less damped. Furthermore, Fig. 3 (b) shows that by only changing the proportional parameter for one converter, the variation tendency is same as shown in Fig. 3 (a), but the variation range is relative small.

Fig. 4 shows pole-zero locus with integral parameter K_{iV} changed from 1 to 300 for containment-based control loop. In Fig. 4 (a), it shows the locus by changing the parameters for four converters simultaneously. In the low frequency region, the zoomed in part of Fig. 4 (a) shows that one dominating pole on the real axis is moving away from the imaginary axis and a pair of poles is moving toward the imaginary axis, which means that the response speed of the system is enhanced. Three poles on the real axis is moving away from the imaginary axis which can increase the dynamic response speed. In the high frequency region, three pairs of poles moving toward the real axis can make the system more damped. In addition, Fig. 4 (b) shows that the system cannot be affected a lot by only changing the parameter from one converter.

Fig. 5 shows pole-zero locus with proportional parameters K_{pI} in *PI* controller for consensus-based current control changed from 0.1 to 1. Fig. 5 (a) shows the locus by changing the parameters for four converters. In the low frequency region, it shows from the zoomed in part that a pair of dominating poles is moving away from the original point making system more damped and transient response more quickly. In the high frequency region, three pairs of poles are moving away from the imaginary axis and towards the real axis which indicate that the response speed is enhanced, and the system is becoming more damped. In addition, Fig. 5 (b) shows the locus by only changing the parameter for one converter. The tendency is same as shown in Fig. 5 (a) and the variation trajectory is shorter than that in Fig. 5 (a).

Fig. 6 shows pole-zero locus considering integral parameters K_{iI} changed from 1 to 600 in *PI* controller for consensus-based current control. Fig. 6 (a) shows the locus by changing the parameters for four converters. In the low frequency region, from the zoomed in part, it shows that a pair of dominating poles is moving towards the imaginary axis which means the system is becoming less damped. In the middle frequency region, three pairs of poles are moving away from the real axis meaning that the system is becoming less damped. Fig. 6 (b) shows the locus by only changing the parameter for one converter. Compared with Fig. 6 (a), it is concluded that only changing parameter for one converter cannot affect the whole stability of the system too much.

The analysis results are concluded in the following as the guideline for system parameter design: for the containment-

This article has been accepted for publication in a future issue of this journal, but has not been fully edited. Content may change prior to final publication. Citation information: DOI 10.1109/TPEL.2018.2878084, IEEE Transactions on Power Electronics

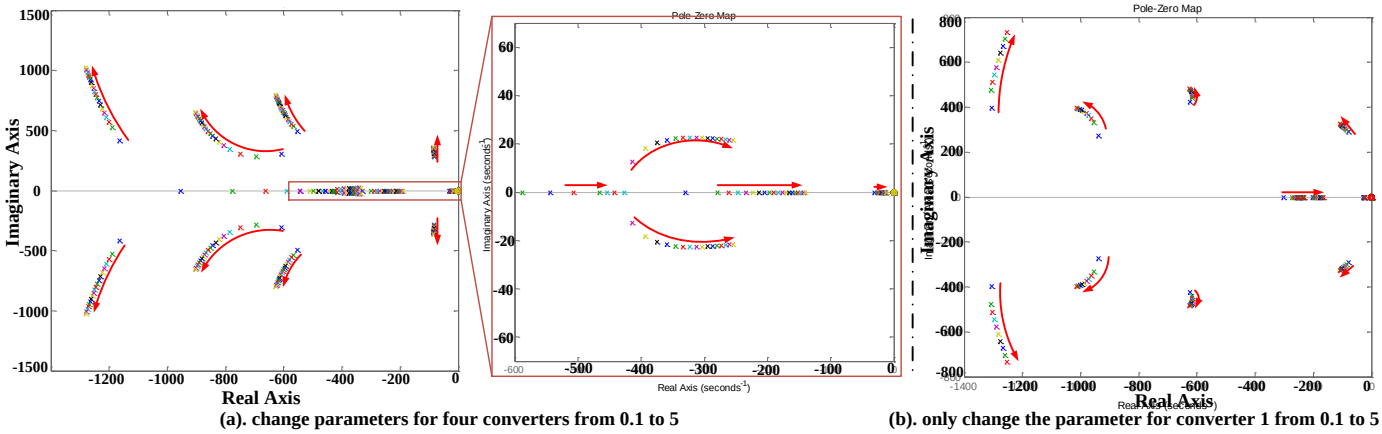

(a). change parameters for four converters from 0.1 to 5 **(b). only change the parameter for converter 1 from 0.1 to 5**

Fig. 3. Pole-zeros locus for K_{pV}.

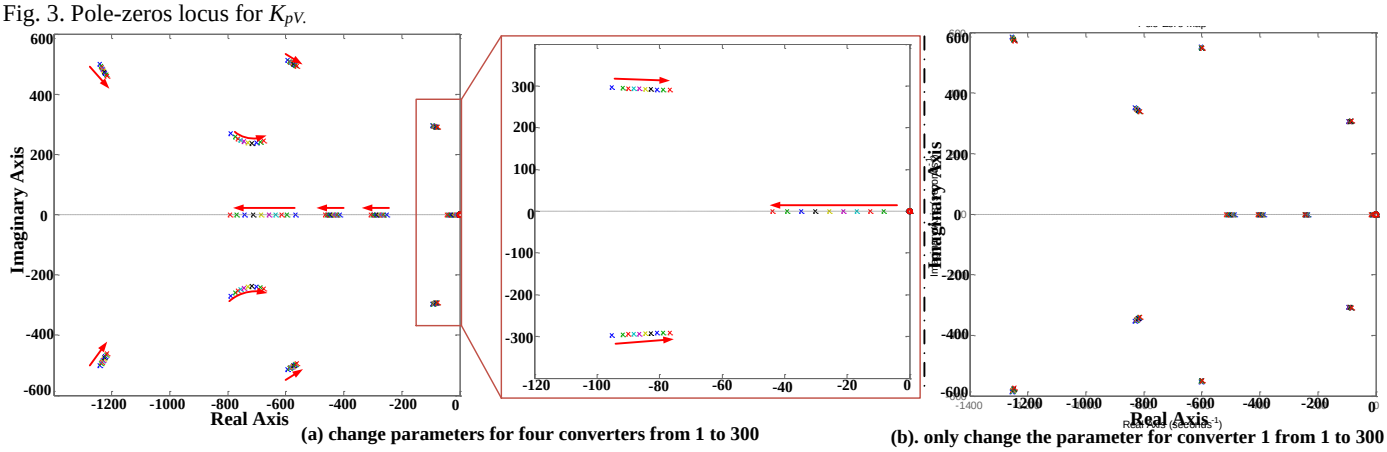

(a) change parameters for four converters from 1 to 300 **(b). only change the parameter for converter 1 from 1 to 300**

Fig. 4. Pole-zeros locus for K_{iV}.

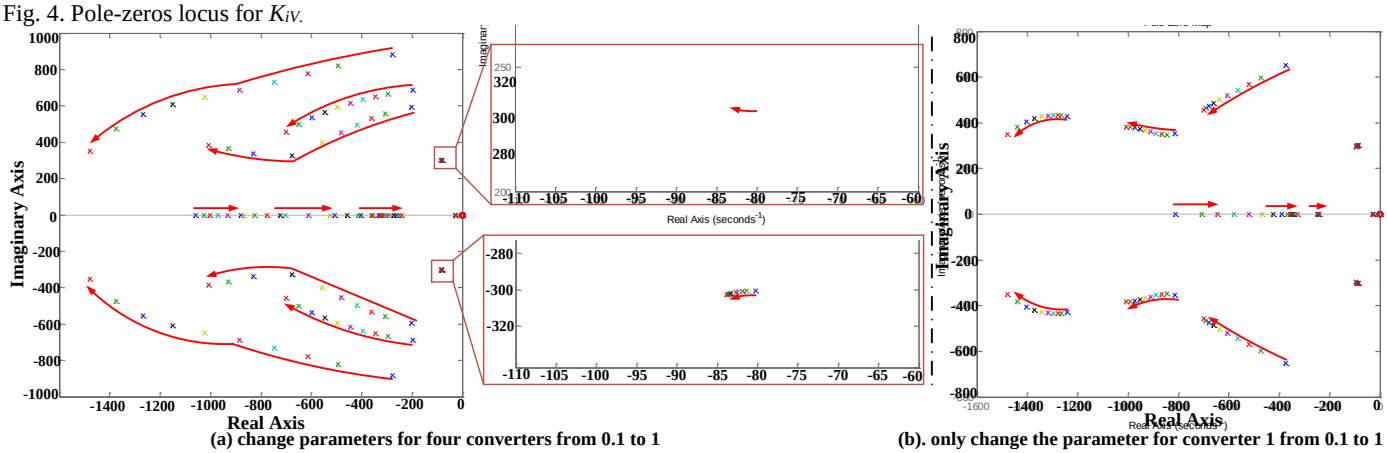

(a) change parameters for four converters from 0.1 to 1 **(b). only change the parameter for converter 1 from 0.1 to 1**

Fig. 5. Pole-zeros locus for K_{pI}.

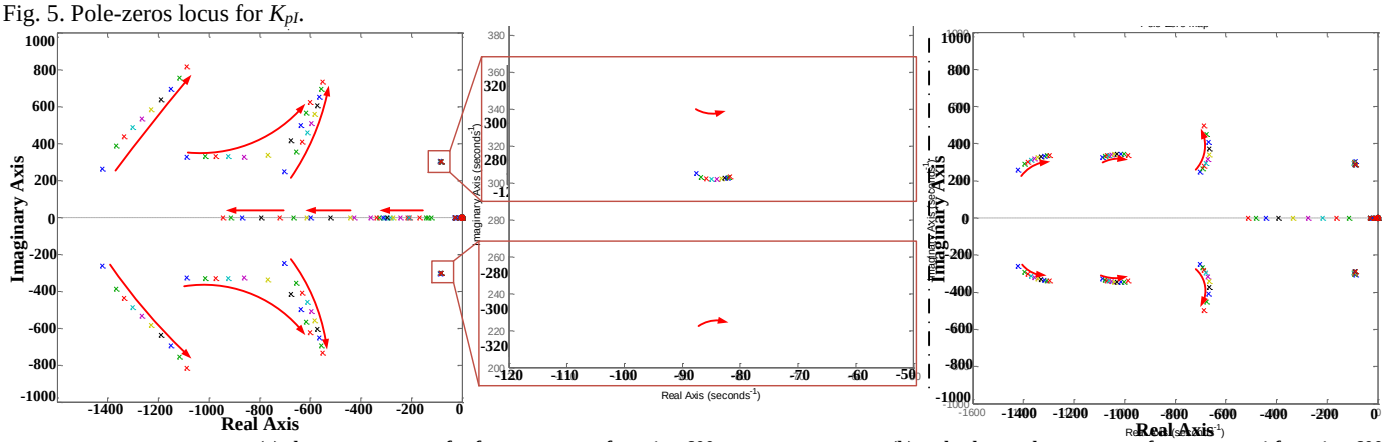

(a) change parameters for four converters from 1 to 600 **(b). only change the parameter for converter 1 from 1 to 600**

Fig. 6. Pole-zeros locus for K_{iI}.

This article has been accepted for publication in a future issue of this journal, but has not been fully edited. Content may change prior to final publication. Citation information: DOI 10.1109/TPEL.2018.2878084, IEEE Transactions on Power Electronics

based controller, by increasing the proportional parameter, the response speed and damping of the system are decreased. Meanwhile, by increasing the integral parameter, the response speed and damping in the system are improved. For the consensus-based controller, by increasing the proportional parameter, the response speed and damping of the system are improved. By increasing the integral parameter, the response speed is improved, but the system is becoming less damped. The whole analysis conclusion is summarized in Table II.

TABLE II. Conclusion of Stability Analysis

Containment-based Controller			Consensus-based Controller		
$\uparrow K_{pV}$	Response speed	$\downarrow$	$\uparrow K_{pI}$	Response speed	$\uparrow$
	Damping	$\downarrow$		Damping	$\uparrow$
$\uparrow K_{iV}$	Response speed	$\uparrow$	$\uparrow K_{iI}$	Response speed	$\uparrow$
	Damping	$\uparrow$		Damping	$\downarrow$

C. Closed-loop Voltage Control Bandwidth Test by tuning Weightings

Fig. 7 shows the close-loop bode diagram by changing the weighting of w_v from 1 to 3. It is illustrated that if the control weighting for containment-based voltage controller is increased, the close-loop control bandwidth can be increased but the system damping at resonance frequency is a little bit decreased. The system stability still cannot be affected.

Here, we provide design guidelines for weighting parameters as follows:

1). Under light to medium load level condition, the control objective is to guarantee accurate current sharing and voltage bound simultaneously, the communication weighting w_c can be chosen a little bit larger.

2). Under heavy load level condition, if the voltage deviations are larger than the standard due to the power flow, the communication weighting w_v should be increased to bound all the voltages in the prescribed range and the current sharing performance should be compromised by decreasing the weighting w_c.

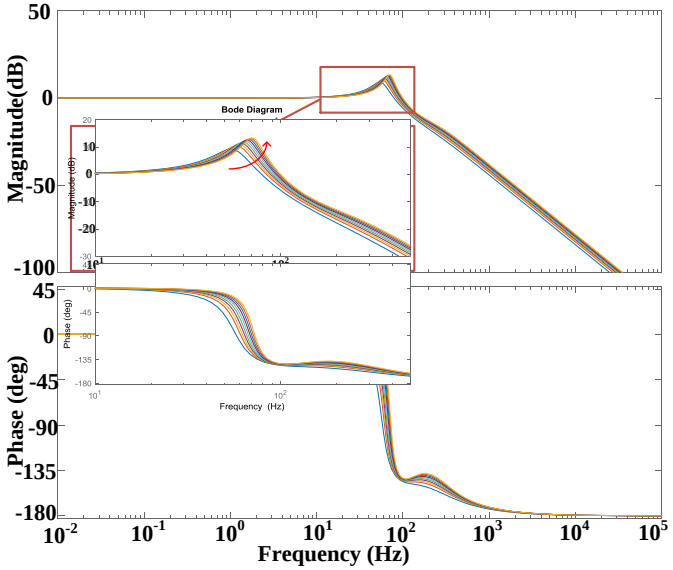

Fig. 7. Close-loop bode diagram by changing the weighting w_v from 1 to 3.

IV. Experimental Tests and Performance Evaluation

The proposed control scheme is implemented and tested in an experimental dc MG setup operated in islanded mode shown in Fig. 8. The setup consists of four parallel-configured dc-dc converters, *LC* filters, different line impedances, electrical loads (resistive load and CPL), dSPACE controller and monitoring platform. The power ratio for four converters rated capacity is 2: 2: 1: 1 from converter 1 to 4. The nominal voltage for the dc MG is *120V*. According to the standard [38], the upper voltage boundary is set as *120*(1+2%)V* which is *122.4V*, while the lower voltage boundary is set as *120*(1-2%)V* which is *117.6V*. The control system parameters are shown in Table III. The experimental results are shown in Fig. 10 - Fig. 19. The communication topology for the proposed controller in the test is given in Fig. 9. Black lines represent the communication between converters, which is used by proposed two controllers. Red lines represent the communication for converters to receive leader information, which is only used by the proposed containment-based voltage controller.

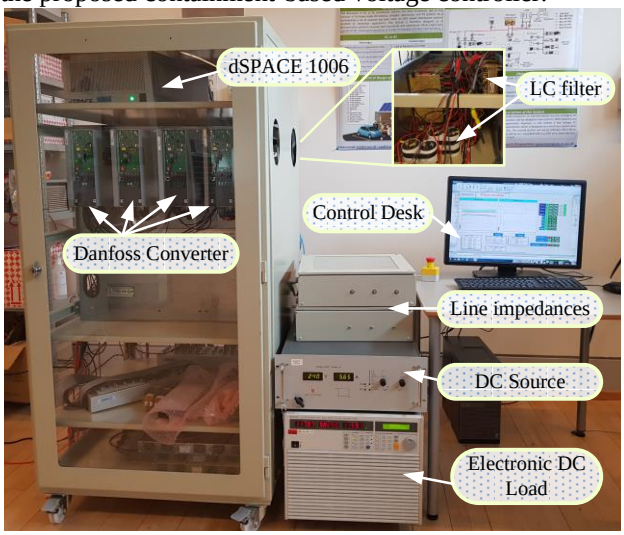

(a). Experimental setup in AAU-Microgrid research laboratory

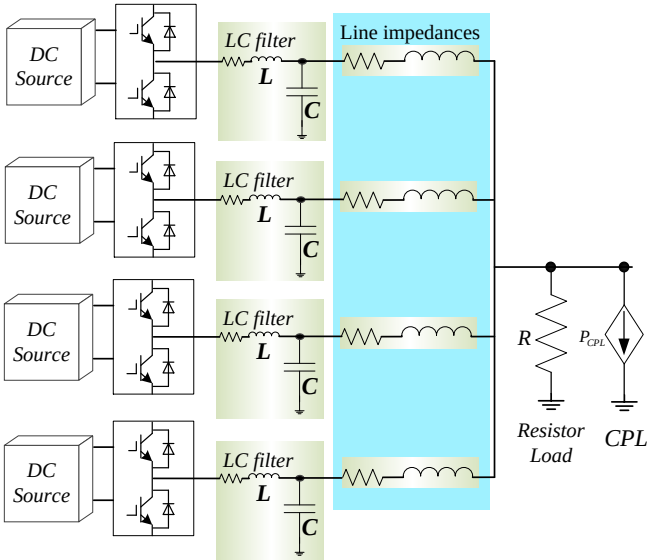

(b). Circuit diagram of testing setup

Fig. 8. Experimental setup and circuit diagram.

This article has been accepted for publication in a future issue of this journal, but has not been fully edited. Content may change prior to final publication. Citation information: DOI 10.1109/TPEL.2018.2878084, IEEE Transactions on Power Electronics

TABLE III. Control system parameters

	Parameters	Value
Electrical Setup Parameters	Filter Inductor	1.8 *mH*
	DC Bus Capacitance	2200 *uF*
	Line impedance for Converter 1	0.7 *Ω*+1.2 *mH*
	Line impedance for Converter 2	1.1 *Ω*+1.5 *mH*
	Line impedance for Converter 3	0.3 *Ω*+1.2 *mH*
	Line impedance for Converter 4	1.9 *Ω*+1.7 *mH*
Inner Current Loop Controller	Current proportional parameter	0.003
	Current integral parameter	0.1
Droop Controller	Droop parameters for Converter 1 and 2 (R_{vir1} and R_{vir2})	1.25
	Droop parameters for Converter 3 and 4 (R_{vir3} and R_{vir4})	2.5
Containment-based Voltage Controller	Weighting for containment-based controller (w_v)	0.2
	Proportional parameter (K_{pVi})	0.5
	Integral parameter (K_{pIi})	90
Consensus-based Current Controller	Weighting of consensus-based controller (w_c)	2.5
	Proportional parameter (K_{pIi})	0.8
	Integral parameter (K_{iIi})	400

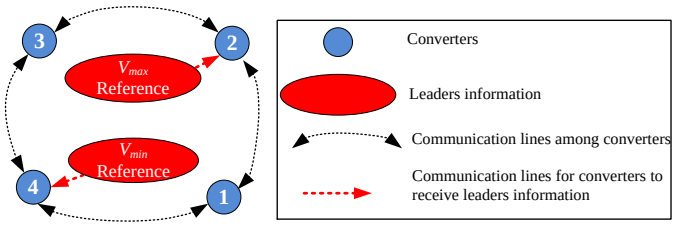

Fig. 9. Communication topology.

A. *Case 1: Control Performance under Resistive Loads*

Studies in this section illustrate the performance of the proposed controllers with resistive loads under different controller tunings. The procedures in the following two tests of Case 1 are same. At the beginning of the test, the load value is *15 Ω* and then, the load value is changed to *12 Ω*, finally the load value is changed back to *15 Ω*.

1) Accurate current sharing and compromised voltage bound regulation

In Fig. 10, at t=*T1*, the proposed controller is activated. Before t=*T1*, the output current cannot be shared and voltage deviations from nominal value exist by using reverse droop control due to the different line impedance effects. After t=*T1*, it is shown in Fig. 10 (a) that the output voltages can be bounded within the boundary while keeping the necessary deviations around nominal value to guarantee the power flow achieving accurate current sharing. At t=*T2* and *T3*, the load is increased and decreased respectively. It is illustrated in Fig. 10 (b), the proposed controller can achieve proportional current sharing accurately. In Fig. 10 (c), the per-unit value can also verify the accuracy of current sharing. In Fig. 10 (d), the total control input from the proposed two controllers is given.

In this sub-case, the weighting for L_V, w_v is *0.2* and the weighting for L_I, w_c is *2.5*. Since the weighting for containment-based voltage controller is chosen small, output voltages are recovered to steady states within *0.7s* after load disturbance, which is a little bit slow. Meanwhile, the current responses are fast without overshoot.

2) Tight voltage regulation with compromised current sharing

In this sub-case, we will show the compromised control performance when the weighting for L_V, w_v, is increased. Here, we set that w_v is 1 which is larger than previous sub-case and w_c is set 2.5 same as before. At t=*T1* and t=*T2*, the load is increased and decreased respectively. By comparison, the voltage performance shown in Fig. 11 (a) is tighter than that shown in Fig. 10 (a). Naturally, the current sharing performance is compromised shown in Fig. 11 (b) and (c) as discussed before. To be mentioned, since the control weighting for containment-based voltage controller is chosen larger than before, the voltage dynamic response is faster than the previous sub-case. It is illustrated in Fig. 11 (a) the output voltages are recovered to steady state within *0.4s* after load disturbances. Meanwhile, the current dynamic responses are fast but with larger overshoots than before. The experimental result is matching with the analysis given in Fig. 7.

B. *Case 2: Control Performance under CPL*

Studies in this section illustrate the performance of the proposed controllers with CPLs under different controller tunings. The procedures in the following two tests of Case 2 is same. During the whole experimental period, the total CPL is changed from *0.5 kW* to *1 kW* and then back to *0.5 kW*.

1) Accuracy current sharing and compromised voltage regulation

The experimental results are given in Fig. 12. In Fig. 12 (a), the voltage can be bounded within the boundary. But, as shown in Fig. 12 (a.1) and (a.2), the dynamic of voltage response is relative slow with CPL disturbances. As shown in Fig. 12 (b) and (c), the current sharing can be guaranteed. In Fig. 12 (d), the control input is provided. In this case, the weightings are same as Case 1-1.

2) Tight voltage regulation with compromised current sharing

In Fig. 13 (a), it is illustrated that the voltage can be tightly bounded within the boundary. Meanwhile, as shown in Fig. 13 (a.1) and (a.2), the dynamic of voltage response is improved. In Fig. 13 (b) and (c), the current sharing performance is compromised because of the tight bounded voltage regulation. In Fig. 13 (d), the control input is given. In this sub-case, the weighting is same as Case 1-2. The voltage dynamic response is faster because of the increased control weighting for the containment-based voltage controller. Meanwhile, the current dynamic responses exist small overshoots. The experimental result is matching with the analysis given in Fig. 7.

To be emphasized, in Case 1-2 and Case 2-2, it is unnecessary to have this compromised control because the load

This article has been accepted for publication in a future issue of this journal, but has not been fully edited. Content may change prior to final publication. Citation information: DOI 10.1109/TPEL.2018.2878084, IEEE Transactions on Power Electronics

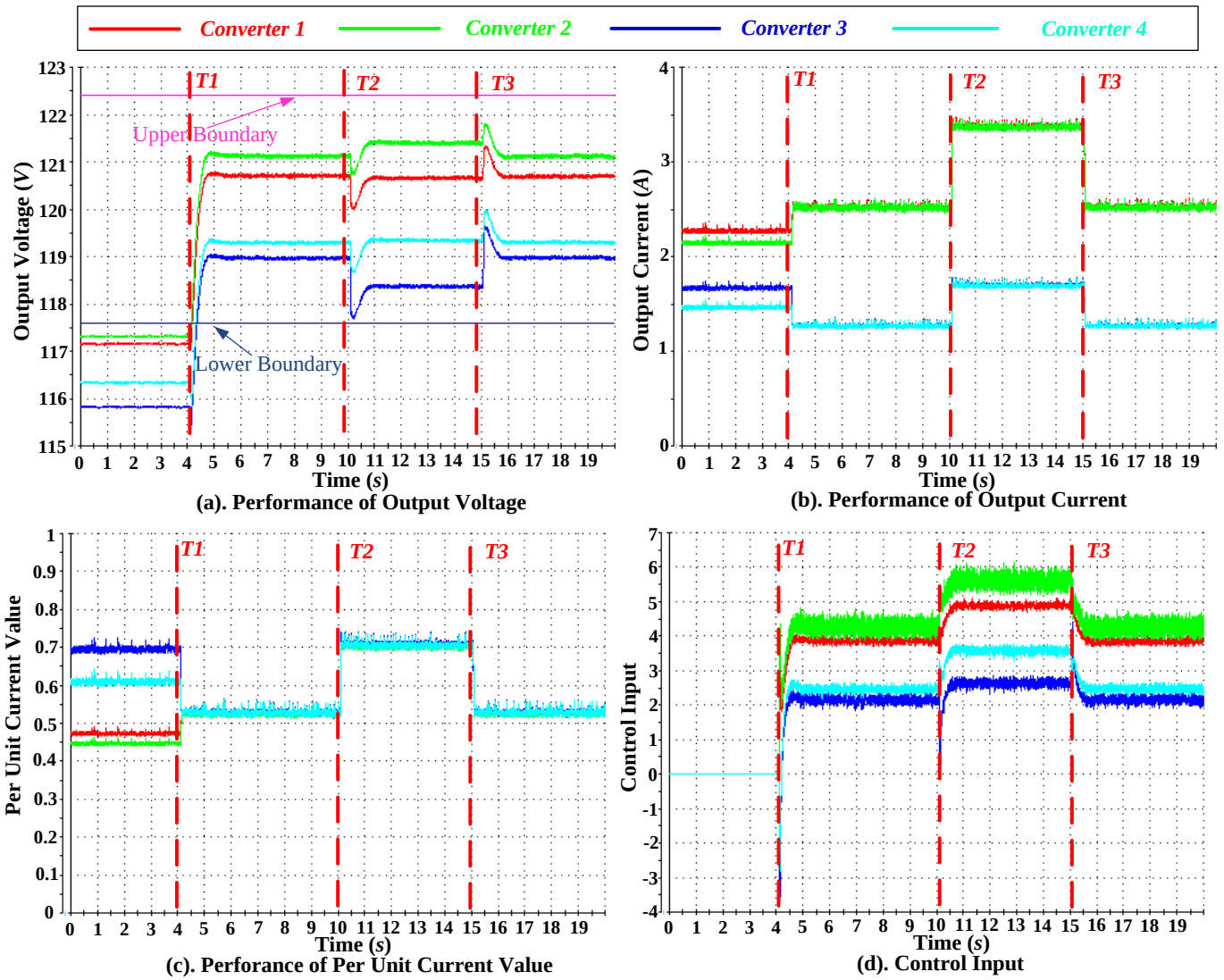

Fig. 10. Control performance with accurate current sharing and compromised voltage regulation under resistive load.

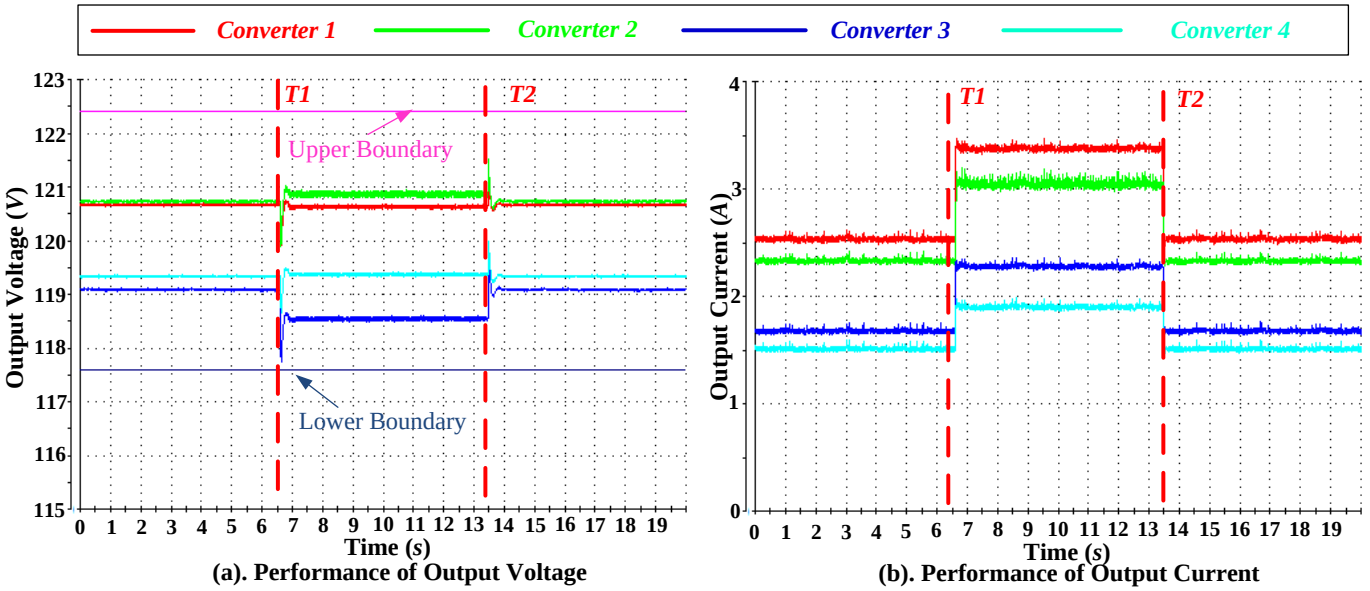

This article has been accepted for publication in a future issue of this journal, but has not been fully edited. Content may change prior to final publication. Citation information: DOI 10.1109/TPEL.2018.2878084, IEEE Transactions on Power Electronics

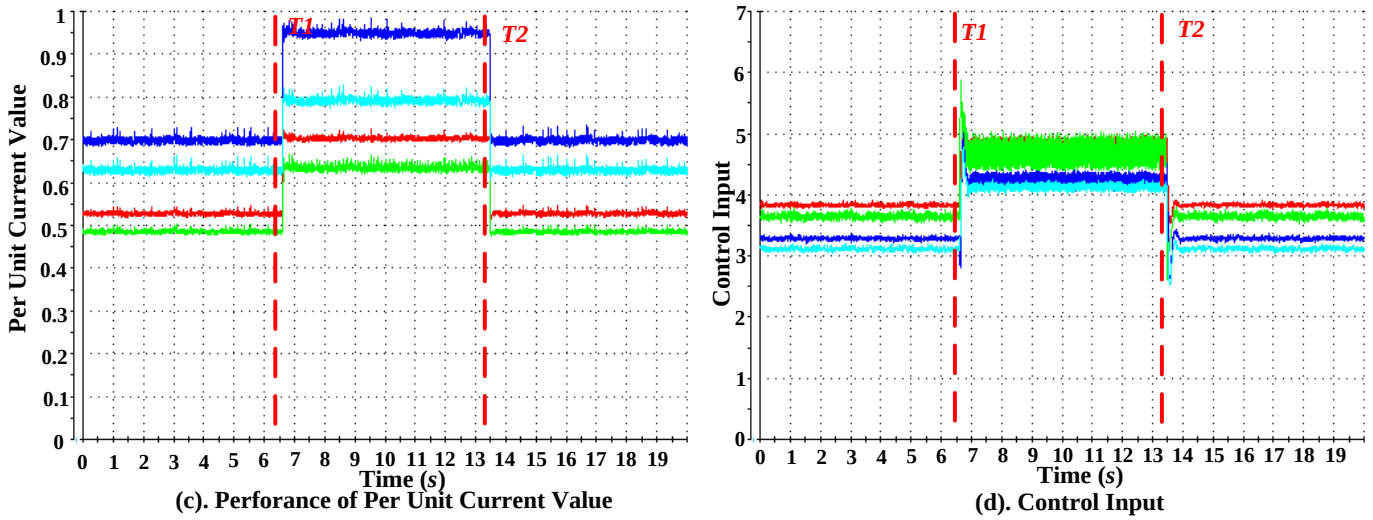

Fig. 11. Control performance with tight voltage regulation and compromised current sharing under resistive load.

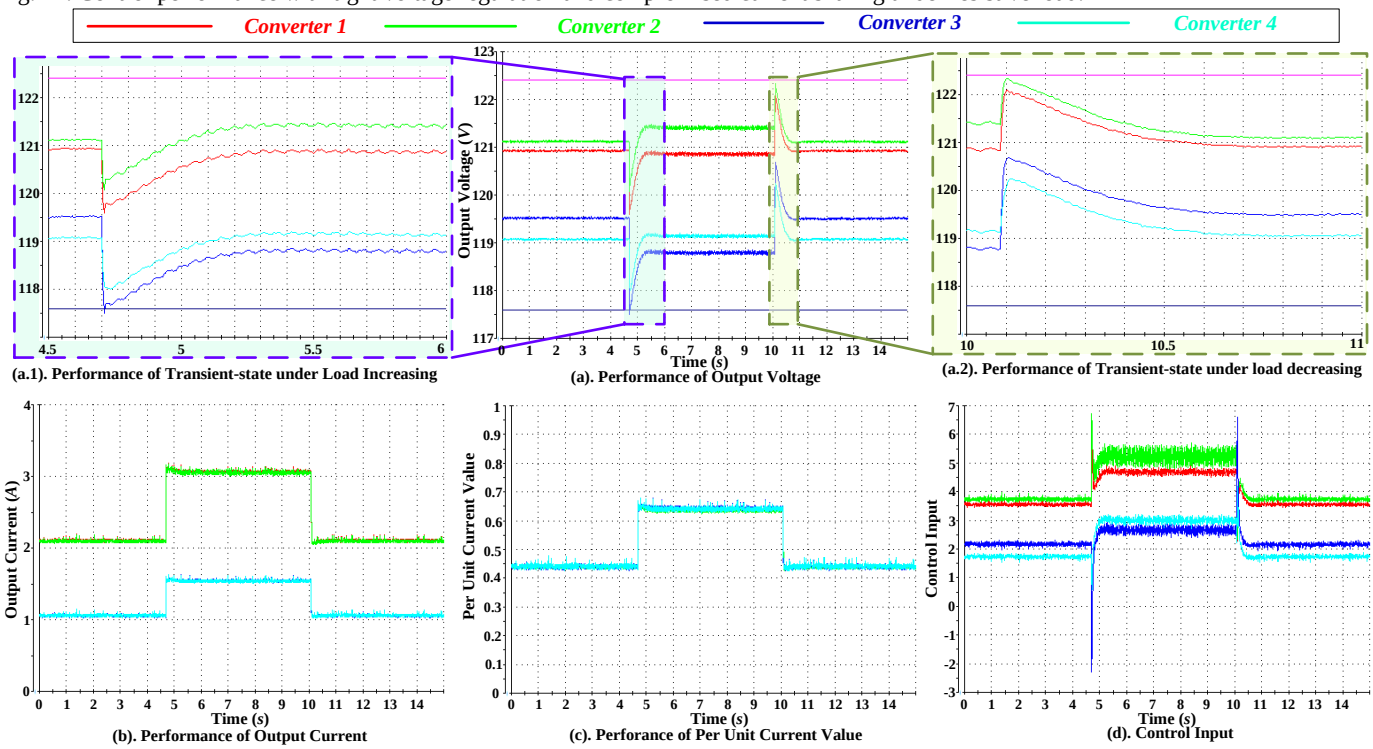

Fig. 12. Control performance with accurate current sharing and compromised voltage regulation under CPL.

condition is not serious. Here, we would like to illustrate the compromised conception. In the following case, the load level will become serious and the necessity about activating the compromised control strategy will be shown.

C. Case 3: Control Performance under serious CPL condition

In the literature, the typical idea to solve the compromised problem is to just control the average voltage and ignore the terminal voltage deviations which means the terminal voltage are uncontrollable in the secondary control level. Under the serious loads condition, even though the average voltage is kept at the nominal value, the terminal voltage deviations would be large, which can affect the power supply quality.

In this case, the effectiveness and comparison are shown under the serious load condition by three cases. The three cases are experiencing same experimental process, during which the CPL is changed from *0.5 kW* to *2.5 kW* with *0.5 kW* step. After the CPL is changed to *2.5 kW*, all the three control methods become unstable. The unstable phenomenon is because of the incremental negative from CPL [13].

Fig. 14 shows the performance with accurate current sharing and compromised voltage regulation by proposed controller. Fig. 15 shows the performance with accurate current sharing and average voltage regulation by control method in [30]. Fig. 16 shows the performance with tighter voltage regulation and compromised current sharing by proposed controller. It can be seen in Fig. 14 and Fig. 15, both the two method can achieve the accurate current sharing with larger voltage deviations. In addition, voltage dynamic responses shown in Fig. 15 is faster than that in Fig. 14 with same amount of overshoots.

This article has been accepted for publication in a future issue of this journal, but has not been fully edited. Content may change prior to final publication. Citation information: DOI 10.1109/TPEL.2018.2878084, IEEE Transactions on Power Electronics

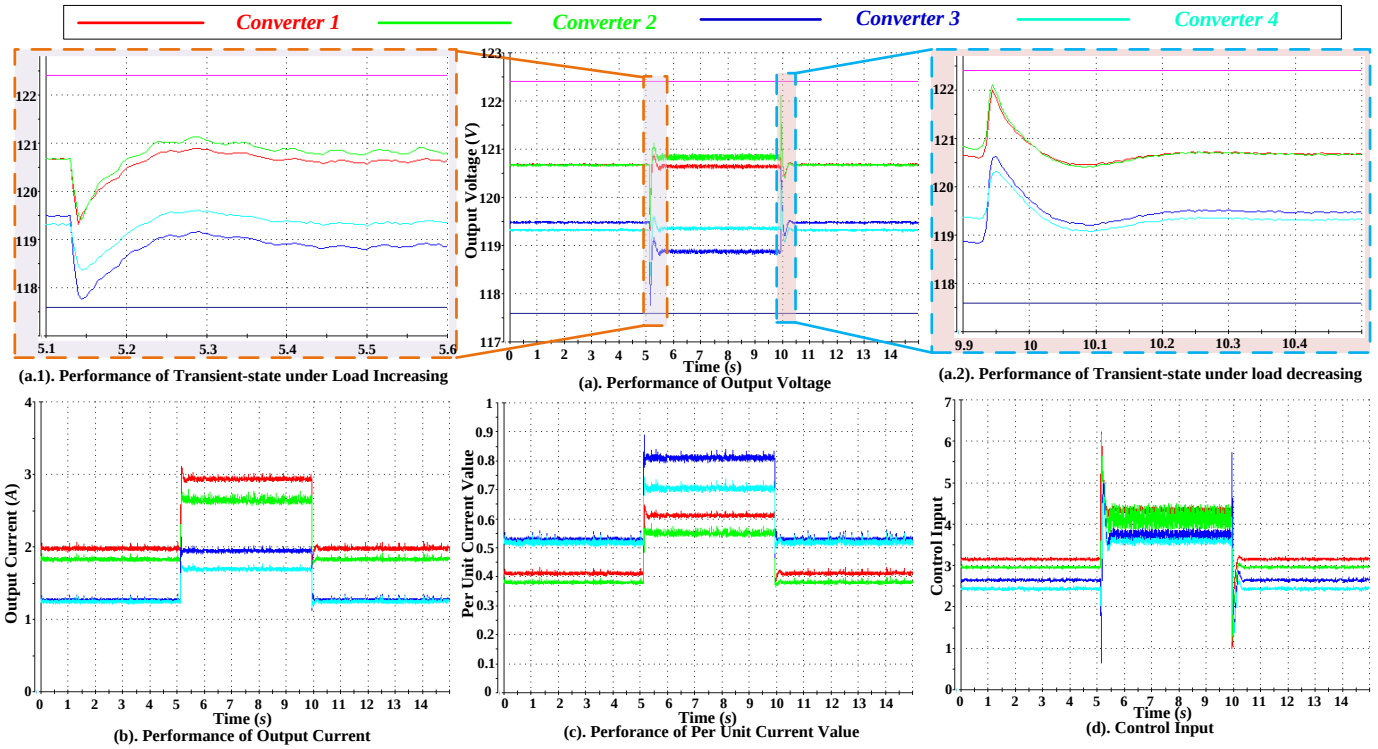

Fig. 13. Control performance with tight voltage regulation and compromised current sharing under CPL.

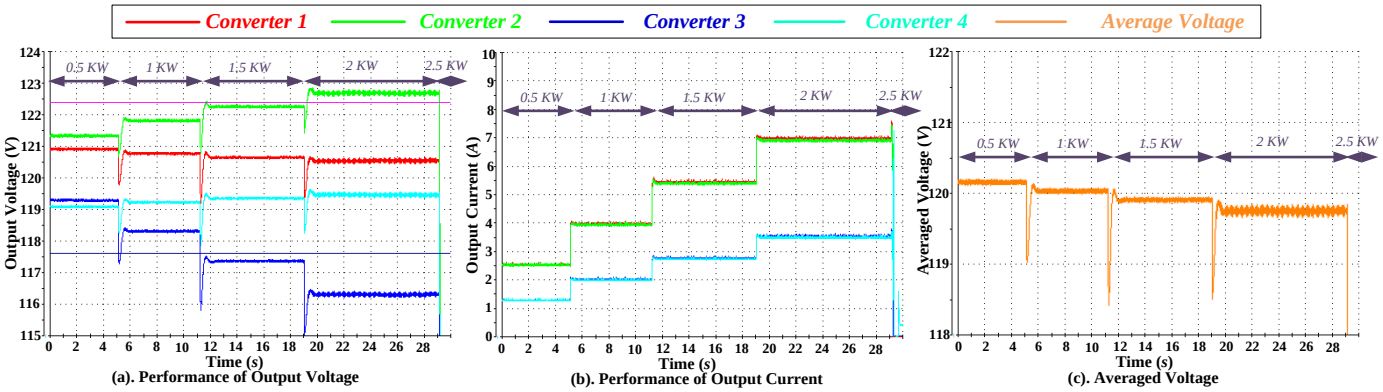

Fig. 14. Control performance with accurate current sharing and compromised voltage regulation by proposed controller.

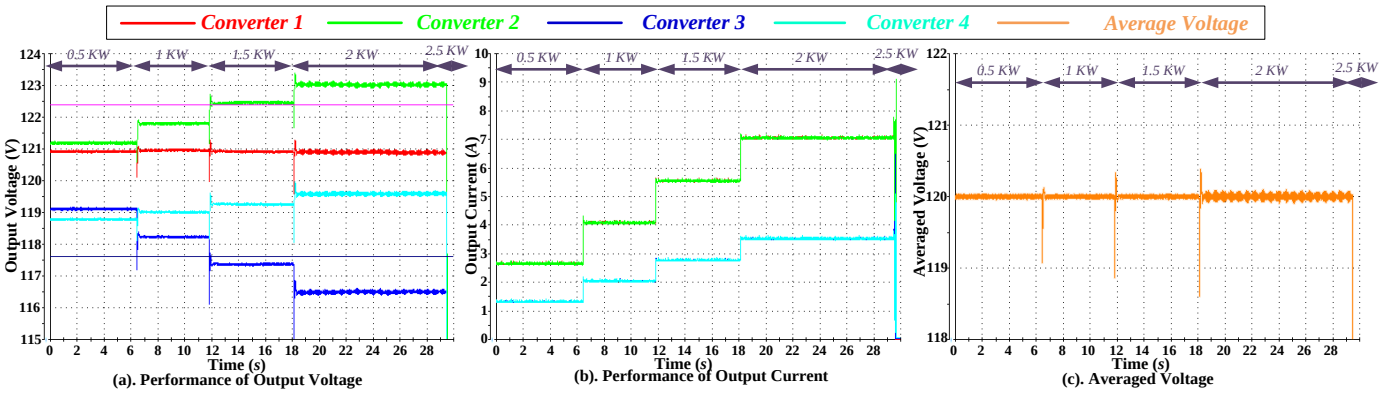

Fig. 15. Control performance with accurate current sharing and average voltage regulation by control method in [30].

Considering the current dynamic responses, Fig. 14 and Fig. 15 illustrate the same performance. The advantage of proposed conception as shown in Fig. 16 is that it provides the freedom to achieve the voltage bound within the standard range guaranteeing the power quality by compromising the current sharing performance rather than only guaranteeing the current sharing performance. Meanwhile, the voltage dynamic in Fig. 16 (a) is faster than that in Fig. 15 (a). The overshoot is also decreased. To be further discussed, during the serious load conditions, the bounding voltage within the necessary range to guarantee the power quality is much more important than accurate proportional current sharing.

This article has been accepted for publication in a future issue of this journal, but has not been fully edited. Content may change prior to final publication. Citation information: DOI 10.1109/TPEL.2018.2878084, IEEE Transactions on Power Electronics

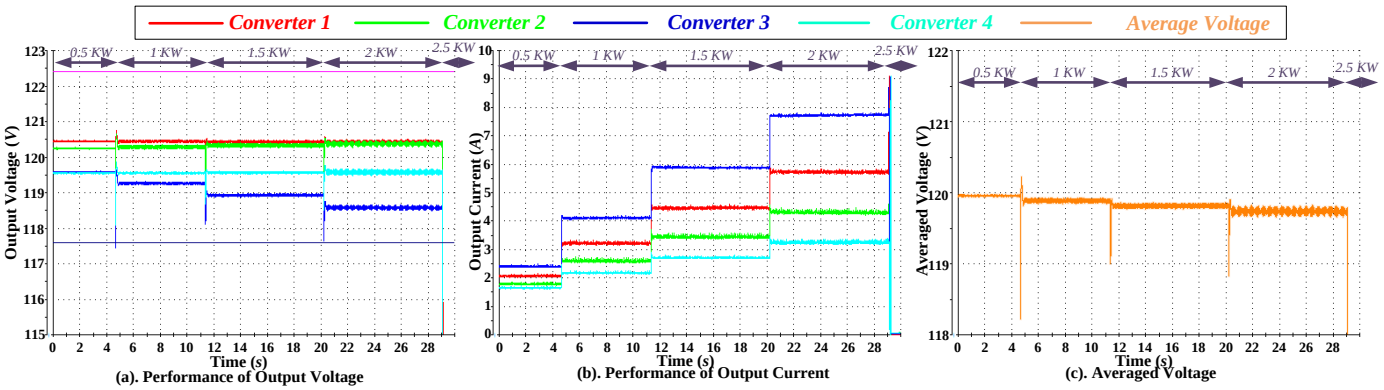

Fig. 16. Control performance with tight voltage regulation and compromised current sharing by proposed controller.

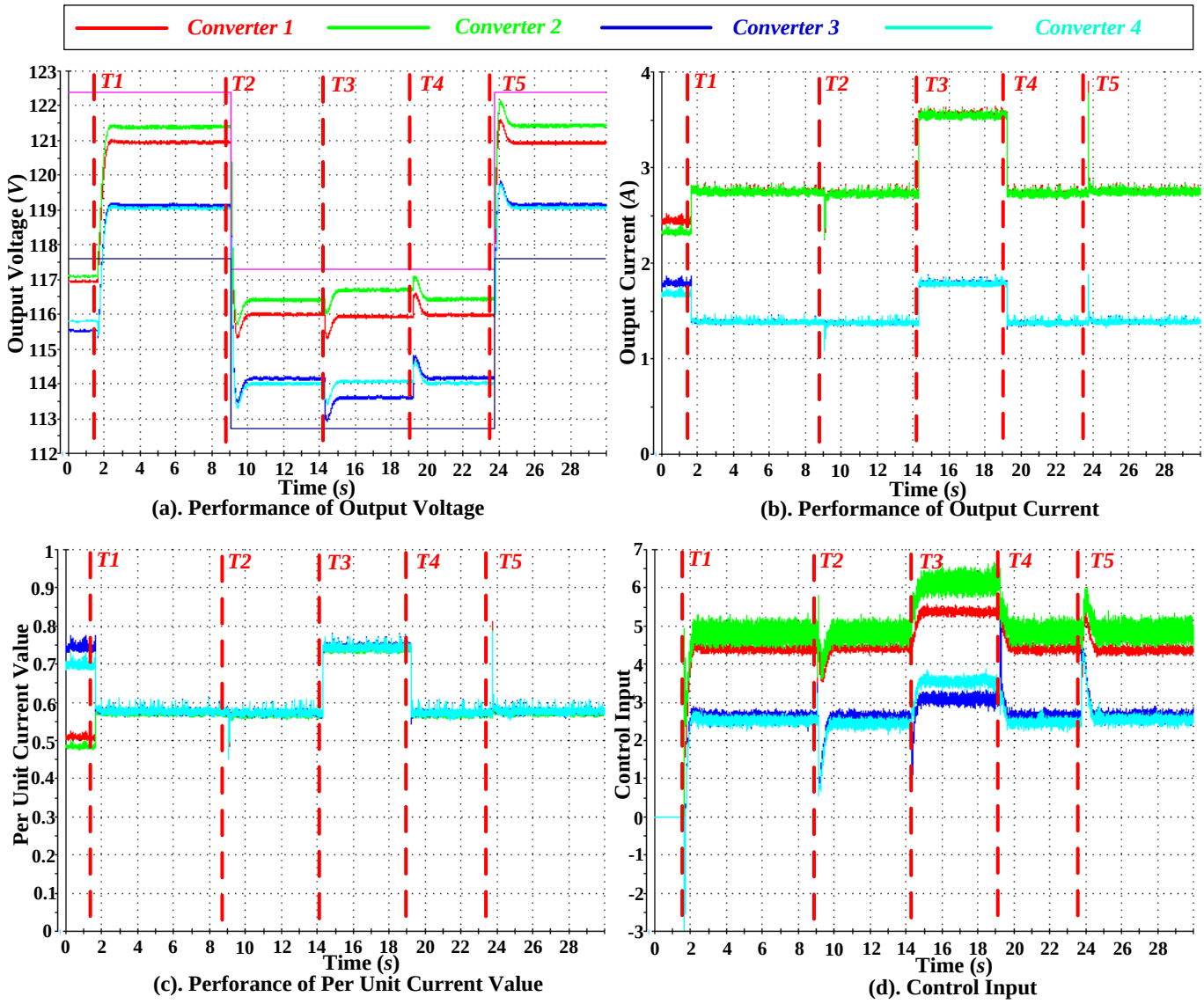

Fig. 17. Control performance with dynamic voltage boundary by proposed controller.

D. Case 4: Control Performance under dynamic voltage range

In this case, the control performance comparison under dynamic voltage range is given by considering the proposed controller, the controllers in [30] and [24].

Fig. 17 shows the performance of proposed controller with dynamic voltage range. At t=*T1*, the proposed controller is activated. Between t=*T2* and *T5*, the voltage boundary is changed. The voltage boundary is changed from $120*(1 \pm 2\%)V$ to $115*(1 \pm 2\%)V$. As shown in Fig. 17 (a), the output voltages can follow the changed voltage boundary very well, while the accurate current sharing is achieved simultaneously as shown in Fig. 17 (b) and (c). During the voltage changing period, the load is increased and decreased at t=*T3* and *T4* respectively. At the beginning, the load value is *15* Ω and it is

This article has been accepted for publication in a future issue of this journal, but has not been fully edited. Content may change prior to final publication. Citation information: DOI 10.1109/TPEL.2018.2878084, IEEE Transactions on Power Electronics

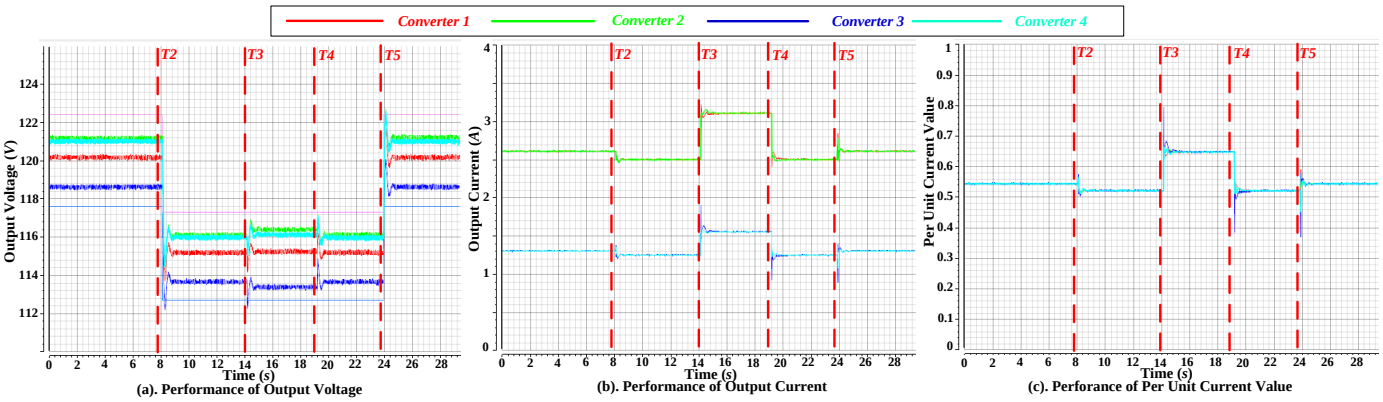

Fig. 18. Control performance with dynamic voltage boundary by controller method in [30].

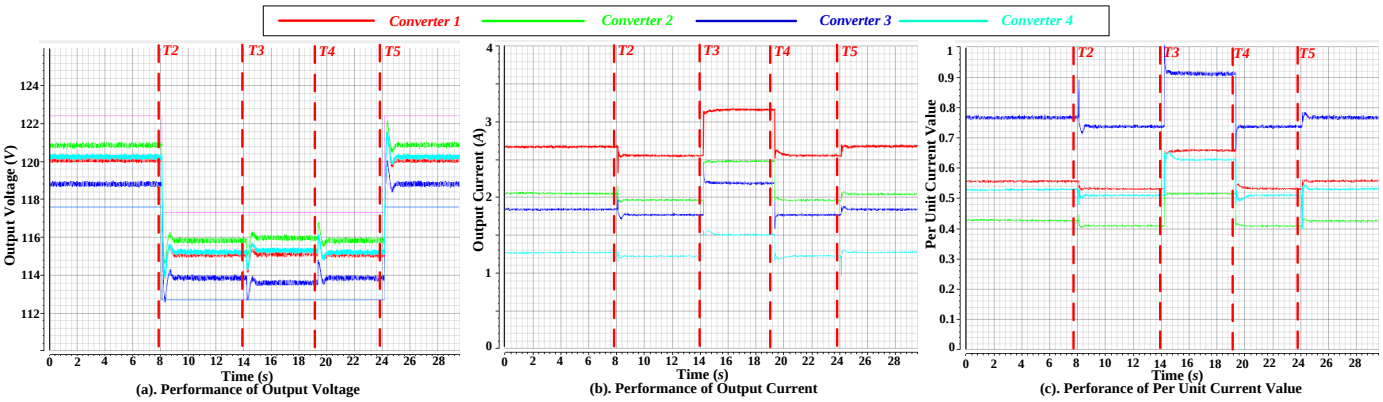

Fig. 19. Control performance with dynamic voltage boundary by control method in [24].

changed to 10 *Ω* at t= *T3*, and then at t=*T4*, it is changed back to *15 Ω*. The accurate current sharing can be guaranteed. At t=*T5*, when the voltage boundary returns to the original range, the performance of bound voltage and accurate current sharing can also be guaranteed.

To be mentioned, the load disturbance is smaller for testing controllers in [24] [30] than that for testing proposed controller. Fig. 18 shows the performance of control method in [30] which considers both the average voltage and accurate current sharing regulations. The experimental procedure is same as before. Between t=*T2* and *T5*, the voltage reference is changed from *120V* to *115V*. At the beginning, the load value is *15 Ω* and it is changed to 12 *Ω* at t= *T3*, and then at t=*T4*, it is changed back to *15 Ω*. Since the load condition is not serious as Case 3, even though only average voltage is controlled, all the output voltages can also stay within the acceptable range. Meanwhile the accurate current sharing can also be achieved. In terms of dynamic responses, the voltage is a little less damped than that shown in Fig. 17 (a) when the voltage reference is changed. Meanwhile, even though the load disturbance is smaller than that for proposed controller, the overshoot in current dynamic response shown in Fig. 18 (b) is a little bit larger than that shown in Fig. 17 (b). Meanwhile, the voltage dynamic responses under load disturbance and voltage reference changing conditions go out of the boundary.

Furthermore, Fig. 19 shows the performance of control method in [24] which consider only the voltage restoration. The idea in [24] about achieving the current sharing is to choose larger droop control parameters to compensate the line impedance differences. If the line impedance differences are large, the performance is not desired. The experimental procedure is still same as before. Between t=*T2* and *T5*, the voltage reference is changed from *120V* to *115V*. At the beginning, the load value is *15 Ω* and it is changed to 12 *Ω* at t= *T3*, and then at t=*T4*, it is changed back to *15 Ω*. By comparing the voltage performance with that in Fig. 17 (a), the voltage dynamic is also less damped shown in Fig. 19 (a). Since there is no further current regulation in the secondary control level, the current sharing is inaccurate as shown in Fig. 19 (b).

V. Conclusion

A distributed coordination control including containment-based voltage controller and consensus-based current controller is proposed to offer the compromised control between voltage bounded regulation and current sharing, which is a highly flexible and reliable operation for islanded dc MG. The compromised conception is achieved by tuning control weightings between two controllers under different system conditions. The proposed compromised controller makes each output voltages controllable in the secondary control sense instead of controlling average voltage value, which mean it provides another degree of freedom for the system. The control parameters guideline is provided by establishing the state-space model of the whole system and analyzing pole-zero loci. Experimental results and comparison between proposed controller and controllers in [24] [30] with different kinds of load conditions are presented to demonstrate the effectiveness of the proposed compromised control scheme.

Reference

[1]. R. Han, H. Wang, Z. Jin, L. Meng and J. M. Guerrero, "Containment-based distributed coordination control to achieve both bounded voltage and precise current sharing in reverse-droop-based DC microgrid," *IEEE*

Energy Conversion Congress and Exposition (ECCE), Cincinnati, OH, 2017, pp. 4121-4127. doi: 10.1109/ECCE.2017.8096716.

[2]. N. Hatziargyriou, H, Asano, R. Iravani, and C. Marnay, "Microgrids," *IEEE Power and Energy Magazine*, vol. 5, no. 4, pp. 78-94, Jul. 2007.

[3]. A. Ipakehi, F. Albuyeh, "Grid of the future," *IEEE Power and Energy Magazine*, vol. 7, no. 2, pp. 52-62, 2009.

[4]. L. Meng, T. Dragicevic, J. Roldan-Perez, J. C. Vasquez, J. M. Guerrero, "Modeling and sensitivity study of consensus algorithm-based distributed hierarchical control for DC microgrid," *IEEE Trans. Smart Grid*, vol. 7, no. 3, pp. 1504-1515, May 2016.

[5]. L. Meng, Q. Shafiee, G. Ferrari Trecate, H. Karimi, D. Fulwani, X. Lu, J. M. Guerrero, "Review on Control of DC Microgrids and Multiple Microgrid Clusters," *IEEE J. Emerg. Sel. Topics in Power Electron*., vol. 5, no. 3, pp. 928-948, Sept. 2017.

[6]. G. Byeon, T. Yoon, S. Oh, and G. Jang, "Energy management strategy of the DC distribution system in buildings using the EV service model," *IEEE Trans. Power Electron*., vol. 28, no. 4, pp. 1544-1554, Apr. 2013.

[7]. F. Chen, R. Burgos, D. Boroyevich, X. Zhang, "Low-frequency common-mode voltage control for systems interconnected with power converters," *IEEE Trans. Ind. Electron*., vol. 64, no. 1, pp. 873-882, Jan. 2017.

[8]. Y. K. Chen, Y. C. Wu, C. C. Song, and Y. S. Chen, "Design and implementation of energy management system with fuzzy control for DC microgrids," *IEEE Trans. Power Electron*., vol. 28, no. 4, pp. 1563-1570, Apr. 2013.

[9]. S. K. Kim, J. H. Jeon, C. G. Cho, J. B. Ahn, and S. H. Kwon, "Dynamic modeling and control of a grid-connected hybrid generation system with versatile power transfer," *IEEE Trans. Ind. Electron*., vol. 55, no. 4, pp. 1677-1688, Apr. 2008.

[10]. M. Kumar, S. C. Srivastava, and S. N. Singh, "Control strategies of a dc microgrid for grid connected and islanded operations," *IEEE Trans. Smart Grid*, vol. 6, no. 4, pp. 1588-1601, Jul. 2015.

[11]. R. Han, L. Meng, G. F. Trecate, E. A. A. Coelho, J. C. Vasquez, and J. M. Guerrero, "Containment and consensus-based distributed coordination control to achieve bounded voltage and precise reactive power sharing in islanded AC microgrids," *IEEE Trans. Ind. Appl*., vol. 53, no. 6, pp. 5187–5199, Nov./Dec. 2017.

[12]. J. W. Simpson-Porco, Q. Shafiee, F. Dorfler, J. C. Vasquez, J. M. Guerrero, and F. Bullo, "Secondary frequency and voltage control of islanded microgrids via distributed averaging," *IEEE Trans. Ind. Electron.*, vol. 58, no. 1, pp. 7025–7038, Nov. 2016.

[13]. R. Han, L. Meng and J. M. Guerrero, "Hybrid droop control strategy applied to grid-supporting converters in DC microgrids: Modeling, design and analysis," *43rd Annual Conference of the IEEE Industrial Electronics Society (IECON)*, 2017, pp. 268-273.

[14]. X. Lu, K. Sun, J. M. Guerrero, J. C. Vasquez, and L. Huang, "State-of-charge balance using adaptive droop control for distributed energy storage system in DC microgrid applications," *IEEE Trans. Ind. Electron*., vol. 61, no. 6, pp. 2804-2815, Jun. 2014.

[15]. X. Zhao, Y. Li, H. Tian, X. Wu, "Energy management strategy of multiple supercapacitors in a dc microgrid using adaptive virtual impedance," *IEEE J. Emerg. Sel. Topics Power Electron*., vol. 4, no. 4, pp. 1174-1185, Dec. 2016.

[16]. S. Peyghami, H. Mokhtari, F. Blaabjerg, "Decentralized Load Sharing in a Low-Voltage Direct Current Microgrid With an Adaptive Droop Approach Based on a Superimposed Frequency," *IEEE J. Emerg. Sel. Topics Power Electron.*, vol. 5, no. 3, pp. 1205-1215, Sep. 2017.

[17]. S. Peyghami, P. Davari, H. Mokhtari, P. C. Loh, F.Blaabjerg, "Synchronverter-Enabled DC Power Sharing Approach for LVDC Microgrids," *IEEE Trans. Power Electron*., vol. 32, no. 10, pp. 8089-8099, Oct. 2017.

[18]. M. Tucci, S. Riverso, G. Ferrari-Trecate, "Line-Independent Plug-and-Play Controllers for Voltage Stabilization in DC Microgrids," *IEEE Trans. Control Systems Technology*, vol. 26, no. 3, pp. 1115-1123, May 2018.

[19]. R. Han, J. M. Guerrero, M. Tucci, A. Martinelli, G. Ferrari-Trecate, "Plug-and-Play Voltage/Current Stabilization DC Microgrid Clusters with Grid-Forming/Feeding Converters," *in Proc. American Control Conference (ACC)*, pp. 5362-5367, 2018.

[20]. J. M. Guerrero, J. C. Vasquez, J. Matas, M. Castilla, L. G. D. Vicuna, and M. Castilla, "Hierarchical control of droop-controlled ac and dc microgrids—A general approach toward standardization," *IEEE Trans. Ind. Electron.*, vol. 58, no. 1, pp. 158-172, Jan. 2011.

[21]. F. Gao, S. Bozhko, G. Asher, P. Wheeler, C. Patel, "An improved voltage compensation approach in a droop-controlled dc power system for the more electric aircraft," *IEEE Trans. Power Electron*., vol. 31, no. 10, pp. 7369-7383, Oct. 2016.

[22]. S. Anand, B. G. Fernandes, and J. M. Guerrero, "Distributed control to ensure proportional load sharing and improve voltage regulation in low-voltage DC microgrids," *IEEE Trans. Power Electron*., vol. 28, no. 4, pp. 1900-1913, Apr. 2013.

[23]. X. Lu, J. M. Guerrero, K. Sun, and J. C. Vasquez, "An improved droop control method for dc microgrids based on low bandwidth communication with dc bus voltage restoration and enhanced current sharing accuracy," *IEEE Trans. Power Electron*., vol. 29, no. 4, pp. 1800-1812, Apr. 2014.

[24]. P. Huang, P. Liu, W. Xiao, and M. Msoursi, "A novel droop-based average voltage sharing control strategy for DC microgrids," *IEEE Trans. Smart Grid*, vol. 6, no. 3, pp. 1096-1106, May 2015.

[25]. M. Mokhtar, M. I. Marei and A. A. El-Sattar, "An Adaptive Droop Control Scheme for DC Microgrids Integrating Sliding Mode Voltage and Current Controlled Boost Converters," *IEEE Trans. Smart Grid*, doi: 10.1109/TSG.2017.2776281.

[26]. P. Wang, X. Lu, X. Yang, W. Wang and D. Xu, "An improved distributed secondary control method for DC microgrids with enhanced dynamic current sharing performance," *IEEE Trans. Power Electron*, vol. 31, no. 9, pp. 6658-6673, Sept. 2016.

[27]. R. Olfati-Saber, J. A. Fax, and R. M. Murray, "Consensus and cooperation in networked multi-agent systems," *Proc. IEEE*, vol. 95, no. 1. Pp. 215-233, Jan. 2007.

[28]. M. Ji, G. Ferrari-Trecate, M. Egerstedt, and A. Buffa, "Containment control in mobile networks," *IEEE Trans. Automatic Control*, vol. 53, no. 8, pp. 1972–1975, Sep. 2008.

[29]. V. Nasirian, A. Davoudi, F. L. Lewis, J. M. Guerrero, "Distributed adaptive droop control for DC distribution system," *IEEE Trans. Energy Convers*., vol. 29, no. 4, pp. 944-956, Feb. 2014.

[30]. V. Nasirian, S. Moayedi, A. Davoudi, and F. L. Lewis, "Distributed cooperative control of DC microgrids," *IEEE Trans. Power Electron*., vol. 30, no. 4, pp. 2288-2303, Apr. 2015.

[31]. S. Sahoo and S. Mishra, "A Distributed Finite-Time Secondary Average Voltage Regulation and Current Sharing Controller for DC Microgrids," *IEEE Trans. Smart Grid*, doi: 10.1109/TSG.2017.2737938.

[32]. M. Cucuzzella, S. Trip, C. De Persis, X. Cheng, A. Ferrara and A. van der Schaft, "A Robust Consensus Algorithm for Current Sharing and Voltage Regulation in DC Microgrids," *IEEE Trans. Control Syst. Technol*., doi: 10.1109/TCST.2018.2834878

[33]. R. Han, L. Meng, J. M. Guerrero, and J. C. Vasquez, "Distributed nonlinear control with event-triggered communication to achieve current-sharing and voltage regulation in DC microgrids," *IEEE Trans. Power Electron*., vol. 33, no. 7, pp. 6416-6433, Jul. 2018.

[34]. L. Ding, Q. Han, L. Wang; E. Sindi, "Distributed Cooperative Optimal Control of DC Microgrids with Communication Delays," *IEEE Trans. Ind. Informat.*, early access, 2018.

[35]. S. Augustine, M. K. Mishra and N. Lakshminarasamma, "Adaptive Droop Control Strategy for Load Sharing and Circulating Current Minimization in Low-Voltage Standalone DC Microgrid," *IEEE Trans. Sustain. Energy*, vol. 6, no. 1, pp. 132-141, Jan. 2015.

[36]. A. Ingle, A. B. Shyam, S. R. Sahoo and S. Anand, "Quality-Index Based Distributed Secondary Controller for a Low-Voltage DC Microgrid," *IEEE Trans. on Ind. Electron.*, vol. 65, no. 9, pp. 7004-7014, Sept. 2018.

[37]. C. Gavriluta, I. Candela, A. Luna, A. G. Exposito, P. Rodriguez, "Hierarchical control of HV-MTDC systems with droop-based primary and OPF-based secondary," *IEEE Trans. Smart Grid*, vol. 6, no. 3, pp. 1502-1510, May 2015.

[38]. R. A. F. Ferreira, H. A. C. Braga, A. A. Ferreira, and P. G. Barbosa, "Analysis of voltage droop control method for DC microgrids with simulink: Modeling and simulation," *in Proc. 10th IEEE/IAS Int. Conf. Ind. Appl*., 2012, pp. 1–6.

[39]. M. Mahmoodi, G. B. Gharehpetian, M. Abedi, and R. Noroozian, "Control systems for independent operation of parallel DG units in dc distribution systems," *in Proc. IEEE Int. Power and Energy Conf*., Nov. 2006, pp. 220-224.

This article has been accepted for publication in a future issue of this journal, but has not been fully edited. Content may change prior to final publication. Citation information: DOI 10.1109/TPEL.2018.2878084, IEEE Transactions on Power Electronics

Renke Han (S'16-M'18) was born in Liaoning, China, in 1991. He received the B.S. degree in Automation, the M.S. degree in Control Theory and Control Engineering both from Northeastern University, Shenyang, Liaoning Province, China, in 2013 and 2015 respectively, and Ph.D. degree in Power Electronics Systems from Aalborg University, Aalborg, Denmark, in 2018.

In 2017, he was a Visiting Scholar with Laboratoire d'Automatique, Ecole polytechnique fédérale de Lausanne (EPFL), Lausanne, Switzerland. He will join in Energy and Power Group, Oxford University, UK, as a postdoctoral researcher in November 2018. His research interests include multi-port converter design, distributed controller for AC and DC microgrid.

He received an outstanding presentation award in Annual Conference of the IEEE Industrial Electronics Society, Italy in 2016 and the Outstanding Master Degree Thesis Award from Liaoning Province, China, in 2014.

Haojie Wang was born in Henan, China, in 1989. He received the B. S. degree in Electrical Engineering and Automation from Zhengzhou University, Zhengzhou, China, and the Ph. D degree in Power System and Automation from North China Electric Power University, Beijing, China, in 2013 and 2018 respectively. He was a guest Ph.D. student with Department of Energy Technology, Aalborg University, Denmark from 2016 to 2017. Now he is a research fellow of Global Energy Interconnection Corporation, Beijing, China. His research interests include DC transmission and distribution, and electric and carbon market.

Zheming Jin (S'15) received the B.S. in Electrical Engineering and M.S. degree in Power Electronics and AC Drive from Beijing Jiaotong University, Beijing, China, in 2013 and 2015, respectively. He is currently woarking towards his Ph.D degree in Power Electronic Systems at Department of Energy Technology, Aalborg University, Denmark. His research interests include control of power electronic converters, stability of power electronic systems, energy storage, dc microgrids and its applications in transportation electrification.

Lexuan Meng (S'13–M'15) received the B.S. degree in electrical engineering and the M.S. degree in electrical machine and apparatus from Nanjing University of Aeronautics and Astronautics, Nanjing, China, in 2009 and 2012, respectively, and the Ph.D. degree in power electronic systems from the Department of Energy Technology, Aalborg University, Aalborg, Denmark, in 2015.

During 2015-2017, he worked as a research fellow in Aalborg University on flywheel energy storage integration project with Maersk Drilling, Denmark. From 2017-2018, he worked in Power Network Demonstration Center, University of Strathclyde, UK, as a research engineer on grid scale energy storage systems. Since 2018 till now, he is an R&D Engineer in FACTS, ABB Sweden, working on FACTS controllers and energy storage systems.

Josep M. Guerrero (S'01-M'04-SM'08-FM'15) received the B.S. degree in telecommunications engineering, the M.S. degree in electronics engineering, and the Ph.D. degree in power electronics from the Technical University of Catalonia, Barcelona, in 1997, 2000 and 2003, respectively. Since 2011, he has been a Full Professor with the Department of Energy Technology, Aalborg University, Denmark, where he is responsible for the Microgrid Research Program (www.microgrids.et.aau.dk). From 2012 he is a guest Professor at the Chinese Academy of Science and the Nanjing University of Aeronautics and Astronautics; from 2014 he is chair Professor in Shandong University; from 2015 he is a distinguished guest Professor in Hunan University; and from 2016 he is a visiting professor fellow at Aston University, UK, and a guest Professor at the Nanjing University of Posts and Telecommunications.

His research interests are oriented to different microgrid aspects, including power electronics, distributed energy-storage systems, hierarchical and cooperative control, energy management systems, smart metering and the internet of things for AC/DC microgrid clusters and islanded minigrids; recently specially focused on maritime microgrids for electrical ships, vessels, ferries and seaports. Prof. Guerrero is an Associate Editor for the IEEE TRANSACTIONS ON POWER ELECTRONICS, He received the best paper award of the IEEE Transactions on Energy Conversion for the period 2014-2015, and the best paper prize of IEEE-PES in 2015. As well, he received the best paper award of the Journal of Power Electronics in 2016. In 2014, 2015, and 2016 he was awarded by Thomson Reuters as Highly Cited Researcher, and in 2015 he was elevated as IEEE Fellow for his contributions on "distributed power systems and microgrids."